January 2022

Efficient Distance Accuracy Estimation Of Real-World Environments In Virtual Reality Head-Mounted Displays

Fatima Kuehn

EFFICIENT DISTANCE ACCURACY ESTIMATION OF REAL-WORLD
ENVIRONMENTS IN VIRTUAL REALITY HEAD-MOUNTED DISPLAYS

by

Fatima El Jamiy Kuehn

Bachelor of Science, Hassan II University, Morocco, 2010

Master of Science, Hassan II University, Morocco, 2012

Master of Science, University of Western Brittany, France, 2012

A Dissertation

Submitted to the Graduate Faculty

of the

University of North Dakota

In partial fulfillment of the requirements

for the degree of

Doctor of Philosophy

Grand Forks, North Dakota
May
2022

Name: Fatima Kuehn

Degree: Doctor of Philosophy

     This document, submitted in partial fulfillment of the requirements for the degree from the University of North Dakota, has been read by the Faculty Advisory Committee under whom the work has been done and is hereby approved.

Ronald Marsh

Ronald Marsh, Ph.D.

Wen-Chen Hu

Wen-Chen Hu, Ph.D.

Emanuel S. Grant

Emanuel Grant, Ph.D.

F. RICHARD FERRARO

Richard Ferraro, Ph.D.

Jeremiah Neubert

Jeremiah Neubert, Ph.D.

_____

     This document is being submitted by the appointed advisory committee as having met all the requirements of the School of Graduate Studies at the University of North Dakota and is hereby approved.

Chris Nelson

Chris Nelson
Dean of the School of Graduate Studies

4/4/2022
_____

Date

iii

Title   Efficient Distance Accuracy Estimation of Real-World Environments in
                 Virtual Reality Head-Mounted Displays

Department   School of Electrical Engineering and Computer Science

Degree   Doctor of Philosophy

In presenting this dissertation in partial fulfillment of the requirements for a graduate degree from the University of North Dakota, I agree that the library of this University shall make it freely available for inspection. I further agree that permission for extensive copying for scholarly purposes may be granted by the professor who supervised my dissertation work or, in his absence, by the Chairperson of the department or the dean of the Graduate School. It is understood that any copying or publication or other use of this dissertation or part thereof for financial gain shall not be allowed without my written permission. It is also understood that due recognition shall be given to me and to the University of North Dakota in any scholarly use which may be made of any material in my Dissertation.

                                                           Fatima E. Kuehn
                                                           April 04, 2022

TABLE OF CONTENTS

LIST OF FIGURES

LIST OF TABLES

ACKNOWLEDGEMENTS

I would like to thank my family, members of my dissertation committee, and friends for their support and understanding. I would especially like to thank Ronald Marsh, my advisor, for his many years of support, and advice. I would also like to give a very special thank you to Naima Kaabouch for her generous advice, guidance, and support throughout my doctoral program.

This dissertation was built upon and drew on previous work of the author. Below is a non-exhaustive list of these works:

- Fatima El Jamiy and Ronald Marsh. A Survey on Depth Perception in Head Mounted Displays: Distance Estimation in Virtual Reality, Augmented Reality and Mixed Reality. IET Image Processing, 8pp, 2019.
- Fatima El Jamiy and Ronald Marsh. Distance estimation in virtual reality and augmented reality: A survey. IEEE International Conference on Electro Information Technology (EIT). IEEE, 2019.
- El Jamiy, Fatima, Ananth N. Ramaseri Chandra, and Ronald Marsh. Distance accuracy of real environments in virtual reality head-mounted displays. IEEE International Conference on Electro Information Technology (EIT). IEEE, 2020.

ABSTRACT

Virtual reality (VR) is a very promising technology with many compelling industrial applications. As many advancements have been made recently to deploy and use VR technology in virtual environments, they are still less mature to be used to render real environments. The current VR systems settings, which are developed for virtual environments rendering, fail to adequately address the challenges of capturing and displaying real-world virtual reality that these systems entail. Before these systems can be used in real life settings, their performance needs to be investigated, more specifically, depth perception and how distances to objects in the rendered scenes are estimated. The perceived depth is influenced by Head Mounted Displays (HMD) that inevitability decrease the virtual content's depth perception. Distances are consistently underestimated in virtual environments (VEs) compared to the real world. The reason behind this underestimation is still not understood. This thesis investigates another version of this kind of system, that to the best of authors knowledge has not been explored by any previous research. Previous research used a computer-generated scene. This work is examining distance estimation in real environments rendered to Head-Mounted Displays, where distance estimations is among the most challenging issues that are still investigated and not fully understood.

This thesis introduces a dual-camera video feed system through a virtual reality head mounted display with two models: a video-based and a static photo-based model, in

which, the purpose is to explore whether the misjudgment of distances in HMDs could be due to a lack of realism, or not, with the use of a real-world scene rendering system. Distance judgments performance in the real world and these two evaluated VE models were compared using protocols already proven to accurately measure real-world distance estimations. An improved model based on enhancing the field of view (FOV) of the displayed scenes to improve distance judgements when displaying real-world VR content to HMDs was developed; allowing to mitigate the limited FOV, which is among the first potential causes of distance underestimation, specially, the mismatch of FOV between the camera and the HMD field of views. The proposed model is using a set of two cameras to generate the video instead of hundreds of input cameras or tens of cameras mounted on a circular rig as previous works from the literature. First Results from the first implementation of this system found that when the model was rendered as static photo-based, the underestimation was less as compared with the live video feed rendering. The video-based (real + HMD) model and the static photo-based (real + photo + HMD) model averaged 80.2% of the actual distance, and 81.4% respectively compared to the Real-World estimations that averaged 92.4%. The improved developed approach (Real + HMD + FOV) was compared to these two models and showed an improvement of 11%, increasing the estimation accuracy from 80% to 91% and reducing the estimation error from 1.29% to 0.56%. This thesis results present strong evidence of the need for novel distance estimation improvements methods for real world VR content systems and provides effective initial work towards this goal.

CHAPTER 1
INTRODUCTION

Virtual Reality (VR) headsets are built to display virtual content. In this thesis, we studied the VR headsets to display a real content instead of a VR content, which is an environment different than the one they are built for. Studying this type of VR technology will allow to explore how far the research in VR can be improved to allow this technology to be used in real life events. VR will be able to be present with surgeons in the operating rooms, firefighters in the extinguish fire area, and more other fields.

As a starting point for this research, we put the prototype of this system. The Oculus Rift DK2 HMD was used, which has two 1920 x 1080 displays with a 90-degree field of view. The real scene was acquired and rendered in real time. Two cameras are used that are streaming live videos to the headset. The two cameras were positioned such as they acquire video as the human eye would. A robot was used to test the first behavior of the system and the two cameras were mounted on the robot to act as the eyes of the robot.

Once the protype was done, it was tested by putting the oculus headset on and driving the robot around. The oculus headset is displaying whatever the robot is seeing through the cameras; however, the person driving had the robot made a right or a left turn before reaching the corner. Another test was done by having few random kids and adults drive the robot around while wearing the Oculus headset in the science day event. We noticed that people drove the robot towards a specific person they know, and they stopped

the robot way before they reach the person to talk to them thinking they are very close to them (usually 2 m before reaching the person). These observations concluded that there is a distance estimation issue involved when displaying real scenes instead of VR scenes on the VR headset. This challenge was approved later by our research and the focus was on improving distance estimations of real environments on virtual reality headsets.

Virtual Reality will become a significant apparatus in real-life tasks and activities. Virtual systems will be handy in dangerous and complex contexts such as firefighting, which is the focus of this thesis. VR is now used in training systems in many different fields. The research questions this thesis is trying to answer are, the potentials and challenges faced to improve VR systems for use in real tasks and not just training. In VR training systems, the distance underestimation may be tolerated since it is just for training purposes. However, this underestimation cannot be tolerated in safety-critical purposes such as saving people's lives or medical surgeries. Typically, VR is used to display a model that was created somewhere else, but there is great promise in using VR to display and render real-world scenes, including photo-based images. As an application, Firefighters use VR systems for training to immerse them in different scenarios mimicking the possible situations they may face in real life. Firefighting and rescuing victims are an extremely dangerous job that puts the life of a firefighter in danger [1].

Virtual Reality research has been increasing in the last years with advances made in this area. Capturing and displaying virtual content has been well developed and still growing, however, capturing and displaying real-world VR content is still not mature [84]. Many factors are involved in the low quality of the rendered scene to HMDs [2-7], and mainly the distance underestimation issue. Existing stitching tools are not convenient for

real-world VR content. Displaying real-world scenes instead of computer-generated scenes has many promising potentials in different fields, such as medicine, firefighting, agriculture and more, and distances underestimation cannot be tolerated in these types of systems.

There are several methods for creation and capturing of real-world VR content [96]. The simplest solution consists of using a conventional camera mounted on a tripod and manually rotating the camera around its optical center [98]. PTZ type motorized cameras (Pan, Tilt, Zoom) are the most-used ones in the industry [97]. The principle is the same, except the camera rotations around its optical center are driven and controlled by a computer. This makes it possible to precisely determine the conditions of the image capture. One of the downsides of this approach (either manual or piloted), is that it takes time to navigate the entire scene. The scene rendering cannot be performed in real time. At a given moment, only a fraction of the scene is seen by the camera [98]. Approaches exist to capture the whole scene in real time. The first is to use omnidirectional camera systems [99]. They can be dioptric or catadioptric. Dioptric camera systems consist of an image sensor and simple reflective elements (wide angle lens or fisheye for example) [100]. In the case of catadioptric camera systems, refractive elements (parabolic, hyperbolic, or elliptical mirror) will be added [101]. This first solution effectively makes it possible to capture the entire scene in real time. However, the image output resolution obtained is generally low, even when using a high-resolution sensor [100].

To increase the resolution, another solution involves using multiple cameras placed in the same location but pointed in different directions. This case allows one to consider, as a first approximation, that the optical center is unique for all the cameras [96]. The more

general solution is to place the different cameras in different places. This technique makes it possible to reconstruct a 3D image of the scene.

In cases where the optical center is unique, the reconstruction of the image obeys the same mathematical rules as the first solution that we have mentioned, i.e., a camera mounted on a tripod, or a motorized camera known as PTZ [102]. The difference between the two camera models mentioned above is the cost of installation, but it allows the whole scene to be viewed with better resolution than omnidirectional cameras.

Mono-panorama generation is another field where many works have been suggested [8] to develop pipelines to create a wider, field-of-view image from different images obtained with variant directions. Most of the 360˚ systems are not stereo panorama systems; hence, they do not offer any depth elements in the output image.

This thesis's goal is to explore distance estimations when real content is displayed in HMDs instead of virtual content. Distances are consistently underestimated in virtual environments (VEs) compared to the real-world [14]. The reason behind this underestimation is still not understood. An initial work [70] investigated another version of this kind of system, that to our knowledge has not been explored by any previous research. Recent research used a computer-generated scene. This work [70] used a dual-camera video feed system through a Virtual Reality Head Mounted Display. The initial work [70] examined distance estimation in real environments rendered to HMDs. Two models were evaluated: a video- based and a photo-based. In this study, we used protocols already proven to accurately measure real-world distance estimations to compare distance judgments performance in the real world and these two evaluated VE models. The purpose was to explore whether the misjudgment of distances in HMDs could be due to a lack of

realism or not, with the use of a real-world scene rendering system. We found that when the model was rendered as static photo-based, the under estimation was less compared with the live video feed rendering. The real HMD model averaged 80.2% of the actual distance, the real photo-based model averaged 81.4%, and the real-world estimations averaged 92.4%.

Additionally, this thesis improves the performance of the real VR content model proposed in the first section by improving the field of view mismatch between the HMD and the camera system. We are proposing a different and low-cost prototype involving only two cameras, which has not been done in previous works. We are presenting a real-world VR content system with a setup of two cameras that allows us to provide an extended field of view with high resolution and generates approximately a complete scene. The two images from the two cameras must be translated to harmonious and coherent output image. We are investigating one of the unanswered questions in previous works, whether the field of view mismatch between the camera and the HMD displays has an impact on the distance estimation performance. The narrow field of view of HMDs is among the biggest challenges in the real-world VR research area. A second question this work is trying to answer is to what extent a two-camera set up scan provide an immersive real-world VR experience. Distance accuracy estimations in an experiment with 18 participants is performed using protocols already proven to accurately measure distance estimations. We compare this approach with the improved field of view with the previous three models we suggested in our previous work. The results have demonstrated that the newly developed approach increased the previous results estimations by 11%. The estimation accuracy was improved from 80% to 91% based on mean absolute error calculations. These results show

that the real VR content system developed provides a strong starting point for the development of even more efficient methods and system requirements to improve distance accuracy for real VR content systems.

CHAPTER 2
BACKGROUND – DEPTH PERCEPTION IN VR

The purpose of virtual reality is to provide a consistent simulation of the realistic world and make interaction between different worlds and objects possible. Perceiving depth and distance correctly in VR is essential, but the perceived depth is influenced by Head Mounted Displays (HMD) that inevitability decrease the virtual content's depth perception. This chapter examines depth perception and Virtual Reality in section 2.1.1 Virtual reality and depth perception are presented in sections 2.1.2 and 2.1.3, respectively. Depth perception in the human visual system is discussed including the different visual cues involved in section 2.1.4. A particular focus will be given in section 2.1.5 on distance estimates methods and techniques in VR and AR.

2.1. Background

2.1.1. Depth perception and virtual reality

Although some studies have investigated the perception of visual objects, few studies that we will go through in the related work section have focused on distance perception. A human perceives the distance of an object and the depth of a scene using several depth cues that are combined to accurately estimate distance and depth, and it has been shown that humans underestimate the distance of distant visual objects (distant objects are located beyond 30m of the observer) and overestimate the distance of near visual objects [14].

Virtual reality systems allow the manipulation of objects in three-dimensional environments. For this, it is essential for VR to manage the quality of its simulations and more importantly the response of the human vision system to these simulations. Virtual reality systems need to accurately create the position of objects in this virtual environment as depth perception is affected by VR headsets and different factors inherent to virtual environments, such as the field of restricted vision or the visualization of unrealistic synthetic images. In VR displays, visual cues are employed to accurately simulate a 3D environment. These depth cues give the brain the necessary information it needs to create an impression of depth. One of the most used techniques in virtual reality to reproduce the depth of an environment is stereoscopy. This technique reproduces certain binocular vision cues. However, it does not accurately reproduce all the visual cues because it decouples convergence and accommodation leading to a discomfort for users [2, 42].

Some users encounter more severe effects, such as motion sickness and dizziness, because of discrepancies between the visual system and the vestibular system. For example, if jumping is performed in a virtual environment, the visual system is informing the brain that the body is jumping while the vestibular system is informing it that the body is not [85]. The way a real scene is perceived is a complex process in which the human visual system uses multiple visual cues along with stereopsis [86]. For an HMD (in nearly all HMDs designs) to reliably render a 3D scene, it should be able to gather and present multiple information cues [70]. Better understanding of depth perception in VR head mounted displays will allow for more control over the scene in the simulated environment as the images are computer generated and their depth information is already known. This

is not necessarily the case when real world scenes are used, as acquired by a camera(s), as the distances to objects may not be known nor correctly captured [70].

2.1.2. Virtual reality

In 1992, Aukstakalnis and Blatner proposed a generic definition of Virtual Reality. They consider VR as a mean for users to visualize and interact with varied and complex computers and data. They introduced three components to consider allowing a user to interact in real time in the virtual environment. These components commonly named the three Is (shown in figure 2.1) are Immersion, Interaction, and Imagination.
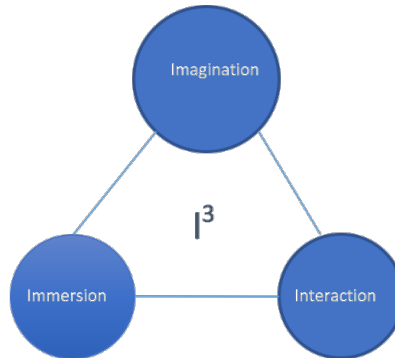
Figure 2. 1. The three Is.

Tisseau [9] defines three mediations of the reality, described in figure 2.2, as a universe of models that proposes the triple mediation of the senses, the action, and the mind. This mediation of the senses allows the **perception** of the real, the mediation of the actions makes it possible to carry out **experiments**, while the mediation of the **mind** allows a mental representation of the reality.

El Jamiy and Marsh [10] explained in their work the basic components of perception and Virtual Reality, and how these components communicate and interact with each other to perform and process depth perception.

More recently, Fuchs et al. [11] proposed two definitions of VR, a technical definition and a functional one:

- Technical definition of VR: VR is a scientific and technical domain exploiting computers and behavioral interfaces to simulate in a virtual world the behavior of 3D entities, which interact in real time with each other, and with one or more pseudo-natural immersion users via sensorimotor channels.
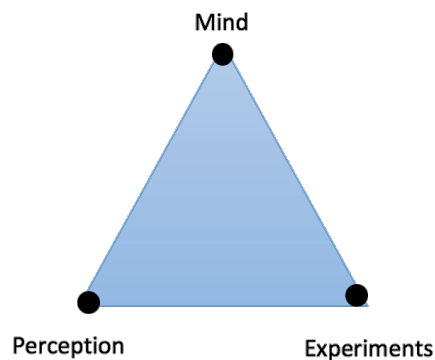
Figure 2. 2. Three mediations of the reality.

- Functional definition of VR: virtual reality will allow users to get out of the physical reality to change (virtually) time, place, and type of interaction: interaction with an environment simulating reality or interaction with an imaginary or symbolic world. Finally, Fuchs et al. [11] proposed a definition that encompasses all definitions. For this purpose, they are based on the goal of VR: "The ultimate goal of VR is to enable one or more sensory-motor and cognitive activity in an artificial world, created digitally which can be imaginary, symbolic, or a simulation of certain aspects of the real world".

To summarize the different definitions of VR and AR, Milgram and Khisino [12]

proposed a unification of concepts by proposing a continuum linking VR and AR. The Virtual Reality Continuum is shown in figure 2.3. The concept of this virtuality continuum refers to the combination of objects shown in any display configuration. Real environments are present at one end of the continuum, at the left, and they refer to environments comprising only real objects. Virtual environments are present at the other end of the continuum, at the right, and they comprise only virtual objects.
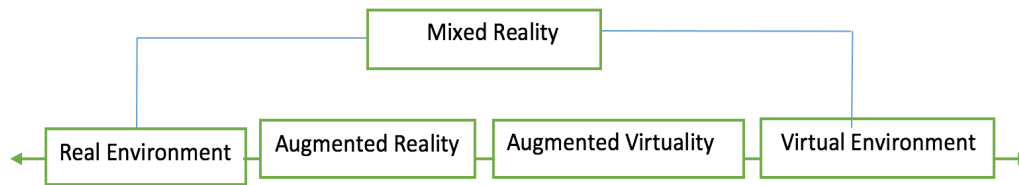
Figure 2. 3. Virtual Reality Continuum.

Applications of virtual reality are characterized by three essential factors: the autonomy of the virtual world, the interaction between the human and the virtual world, and the immersion of the human in the virtual world. The study presented in this work focuses on the third characteristic: immersion. VR provides users with a feeling of presence: users feel like they are in the VR, rather than in the room incorporating the simulator. For many years, virtual reality was limited to visual rendering of computer-generated images on a stereoscopic screen. Nowadays, several modalities are used such as vision, audition, and touch. Virtual reality allows a dynamic, interactive, immersive, and multimodal rendering of a virtual environment.

2.1.2.1.   Visual interfaces

The distance of a real visual source is usually underestimated. Even so, Willemsen et al. [3] and Loomis and Knapp [13] have shown a greater compression of the target egocentric

distance in a VR compared to a real environment, Murgia and Sharkey [14] have shown a coherence in the perception of the distance between real and virtual visual environments.

These results suggest that virtual reality can be used to estimate the egocentric distance of visual objects. To make the most of the capabilities of the human visual system, the capacity of visual interfaces used in virtual reality is evaluated according to four characteristics based on those introduced by Fuchs [15]:

- its horizontal and vertical field of vision,
- the presence of a stereoscopic rendering, which improves depth perception,
- visual content
- the stability of the visual environment.

The Cave Automatic Virtual Environment (CAVE) was the first system designed using this type of interface. Another type of visual interface allowing a large field of view is the Head-Mounted Display (HMD). The HMD interface has the advantage of totally immersing the observer in the virtual scene. In addition, HMDs require little space because subjects can be placed in a room that has not been specifically designed to implement virtual reality applications.

Although Creem-Regehr et al. [16] showed that the field of view has no influence on the perception of distance in a real environment, test subjects performed better with a visual interface of the CAVE type as compared to a single screen appearing in front of the camera [17]. Indeed, an environment of the CAVE type allows a peripheral vision. In addition, according to Wu et al. [18], it is the continuity of the ground between the real environment (test room) and the virtual environment that allows for a better estimate of the

distance. Thus, for Plumert et al. [19], the use of a CAVE system made it possible to obtain identical performances (i.e., identical underestimation) to a real environment.

2.1.2.2. Visual content

The visual scene can be computer generated or formed from realistic images. However, according to Willemsen and Gooch [20], both types of images produce the same depth perception. According to these authors, it is the visual rendering system (in this case, a VR headset HMD like the Oculus Rift shown in figure 2.4) that is causing the distance underestimation from a real environment. Moreover, in the case where the virtual environment does not represent a real environment, the amount of information seems to have an influence on the perception of egocentric distance. Murgia and Sharkey [14] show that it is the perspective visual cue that seems to have the greatest influence in a virtual environment, and the lack of this cue leads to a decrease in perceived egocentric distance.

Figure 2. 4. Oculus Rift.

The visual scene can either (i) reproduce all or part of the real environment surrounding the observer, or (ii) correspond to a different virtual environment. HMDs allow one to completely decouple the real environment from the virtual environment. Interrante et al. [5] show that a reproduction of an accurate test room allows for a better estimate of egocentric distance.

2.1.3. Depth perception

Accurate estimation of the distance of objects around us is an essential task of our life. For example, it is vital to know the position of a car and how far we are from it when we are about to cross the street. The perception of the outside world, beyond what is at hand is essentially done through two senses: vision and audition and several studies have shown that vision allows a better location of objects in space than audition [21,22].

Many studies have shown that the target egocentric distance is underestimated [23] and this effect had already been detected by Bekesy and Wever [24]. According to Cutting and Vishton [25], the visual environment of an observer can be divided into three subspaces (see f 2.1): the personal space (up to 2m), the action space (between 2 and 30m) and the distant space (beyond 30m). The literature shows that the distance perception is not identical for each subspace. The distance egocentric is:

• underestimated for objects in the space of action and distant space,

• over-estimated for objects in personal space.

In the absence of distance cues, the subject locates the object at a "default" distance, called dark vergence in visual perception, which is located 1.9m from the subject.

Table 2. 1. The visual space types.

The personal space	Up to 2m, targets can be grasped and handled by hands
The action space	Between 2 and 30m. Within this subspace, actions such as walking and running are possible and allows to grasp objects, throw them and also communicate and carry out conversations.
The distant space	Beyond 30m; in this subspace, running and walking are performed and includes targets that can be reached or moved away from.

2.1.4. Perception and depth cues

The process of creating a real description of the real world is a complex system that involve many computing resources. The operation involving the generation of the image on the human eye and its processing by the brain is not completely understood [87]. Creating a virtual environment system able to have a full simulation of the human visual system is not reachable yet, because many input parameters called depth cues are involved in the computation of depth and distance and are not yet fully discerned.

Visual perception has been active research for a decade with a lot of work done to demystify the depth perception mechanism. Depth perception occurs from the incorporation of various visual depth cues. Research done to understand depth perception process involves studying the depth cues, the visual characteristics, and the mechanism of how these parameters are performed by the human visual system and integrated together by the brain to generate the representation of the visual real world.

As mentioned by Loomis [26], Loomis et. Al [27], and Loomis et. Al [28], they tried to explain and run experiments to understand how this visual function works. They examined the process of mapping between real space and its creation, the relationship between the perceived space and motor action.

Depth cues involved in the human visual system perception fall into two categories, as shown in figure 2.5:

- **Proprioceptive cues (accommodation and convergence)** are adjusted by the visual system. These cues are reliable at close range (a few meters).
- Visual cues composed of **binocular cues, monocular cues, and Dynamic cues (see sections below)**.
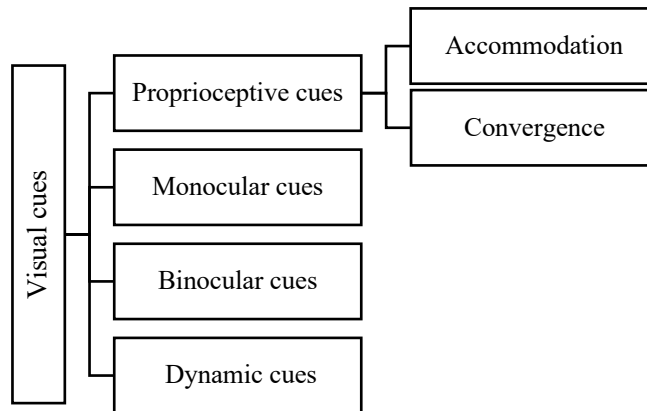
Figure 2. 5. Depth cues categories.

2.1.4.1. Proprioceptive cues

Proprioceptive cues, convergence, and accommodation are the cues related to active perception of the visual scene. These provide accurate depth information mainly for objects in personal space (up to 2m).

Convergence corresponds to the orientation of the visual axis (light beams from the object and arriving at the retina) from each eye to the same target, the point of fixation. So, each eye perceives a slightly different image of the same visual scene. These two slightly different images of the same object allow to extract depth information. Accommodation is related to convergence. However, this relation is bounded and limited, a certain degree of independence exists between the two cues according to Morgan [29]. The change of convergence reflexively causes accommodation on the new fixation point. Accommodation is achieved by the modification of the lens. In the absence of a visual object, an observer tends to accommodate at a distance of 75 cm, called dark focus according to Patterson [30].

2.1.4.2. Monocular cues

It is important to note that with only one eye, the human interprets the image received and deduces notions of depth through monocular cues. These are learned unconsciously, from the youngest age. This section introduces different monocular visual cues.

- The variations of light and the shadows on the objects increase the "relief" [88].

- Outside, the variation in visibility due to the degree of transparency of the atmospheric layer called optical thickness gives depth information on big distances (beyond 100m). It is defined by the diffused fraction of light or absorbed by the components of the layer passed through. These components correspond to particles suspended in the air (dust and pollution).

- The perspective gives information of the three-dimensional space: soil, walls, ceiling, objects [89]. This cue, used in painting since the time of the Renaissance allows to perceive the depth in a visual scene represented in two dimensions.

- The occultation of an object by another makes it possible to relatively locate the objects in depth [90]. Occultation is a visual cue of relative distance.

- The relative size of the object is a main cue in perception of distance [91]. The size decreases with distance. However, without information on the dimensions of the object, the size remains a perception index of relative distance.

- The finesse of the textures gives a complementary information of the depth [92]. The texture of a surface is perceived more clearly if the surface is positioned at low depth. This is the texture gradient.

- Image blur, called also atmospheric perspective, which appears in the vision of certain vast spaces. Objects located far from the observer have contours that appear

blurred [93]. The more an object is far from the observer (over long distances), the more its outlines become blurred. Some hills appear clearer and fuzzier than others, they are the furthest away. The case also when we are on a mountain, and we look in the distance. Some research worked on the development of tunable focus cues and a defocus blur to deduce depth perception.

2.1.4.3. Dynamic cues

The visual cues vary depending on the position of the observer. These variations due to translation or rotation of the observer increases the amount of information available. The movements of the observer or objects in the visual scene induce a new cue: The parallax of motion corresponds to the movements of the observer relative to objects, or the movements of objects between them [94]. These movements can be a translation or a rotation. This cue induces a change in the position of the object in the scene and thus a modification of the visual cues.

Our perception of the world is multisensory: multiple cues of perception are available for the subject. The position of an object in space is the result of the integration by the brain of different sensory information. For example, the cognitive treatment of binocular disparity is strongly influenced by the angle of convergence of the two eyes. However, not all cues have the same contribution in this integration according to Landy et al. [31]. It is based on both structural (spatial and temporal alignment of visual cues) and cognitive cues (semantic coherence of visual cues) [32].

Subjects combine different cues to determine the precise position of the object. An integration process was developed by Landy et al. [31] and modified by Philbeck and Loomis [33] for the visual modality. This visual modality process happens in four stages, as shown in figure 2.6 (see below for details of each stage).

Figure 2. 6. Visual modality stages.

Perception / Adjustment

The visual scene is perceived by the subject. The subject determines the depth cues. In parallel, there is an adjustment of the perception according to different external factors. These factors are related to the methodology (verbal description, triangulation), the subject's knowledge of the subject and the environment, and the subject's movements (variations of the cues). Andre and Rogers [34] describe those two processes for estimating egocentric distance coexist: the first (ambient) when the subject must estimate the distance that separates him from an object, and the second (focal) when the subject must actively move to the object.

Comparison

Each cue produces its own estimation of distance. The estimations are then compared in pairs [33].

Judgment

A coefficient is assigned to each estimation quantifying the degree of reliability of the perceived cue. These coefficients are determined from external factors and the influence of each cue [33]. Then, all estimations are integrated into a single estimation of the distance of the object (weak fusion process).

Description

The final value corresponds to a description by the subject of the distance perceived according to the methodology used [33].

Visual cues must remain consistent to produce a single source. When these cues are coherent, they lead to an improvement of depth perception. However, in case of conflicting cues (i.e., not coincidental), they lead to a deterioration in perception, i.e., a decrease in accuracy or a deviation to the position of the cue having the most influence on perception [33].

2.1.5. Depth perception protocols

Depth perception process is an unseen cognitive condition and therefore not attainable directly. Using human capacity to compare between things and quantities, research use egocentric distance comparison to judge depth and distance. According to Cutting and Vishton [25], human distance perception is still not completely discerned even after being considerably studied for almost 100 years. The work done over these years helped in demystifying the most basics to comprehend how distance perception works, and most importantly, generated different experimental measurements and protocols. Measuring distance perception is challenging, it cannot be assessed directly because it is a conscious event, and for that reason, the different experimental techniques include quantifying judgments reported by a subject. The main employed methods to measure distance perception include matching task, verbal reporting, and bisection task. In the matching task, the position of a marker in one orientation is adjusted by a subject to correspond to the distance to an objective. In verbal reporting, subjects use a unit of measurements to give and communicate a distance between them and an object. Whereas, in the bisection task, subjects position a mark in the middle of the distance between them and an object.

Thompson et al. [7] discuss other measurement protocols that are also used to quantify the distance parameter blindly, such as blind walking and blind reaching where the subject try to reach an already seen object with eyes covered.

2.1.5.1. Blind walking method

Thompson et al. [7] specifies that blind walking is considered as the main technique used to assess and quantify distance judgments. In this technique, a subject sees an object and then walk towards it with covered eyes. Waller and Richardson work [35] demonstrate blind walking's dominance as a technique, where their experiments showed the performance of this task by subjects with a marked precision. Furthermore, the perceived distance measured without bias in the real world is proven by the blind walking task that is mostly close to the expected value. Nevertheless, Loomis and Philbeck [36] showed that blind walking does not perform well in distances beyond 20 m. It seems that the method has limited distance performance.

2.1.5.2. Verbal Reporting method

Verbal reporting is used to assess distance for the three types of subspaces, personal, action and distant distances. The subject in this technique is in a motionless position. Da Silva [23] utilizes verbal reporting to investigate distances up to 9 km. But different research has shown that distances with verbal reports are commonly compressed, and Loomis and Philbeck [36] investigated more the impact of cognitive ability on verbal reporting method. The reported distance by verbal reporting is considered objective since they do not require arranging and controlling objects by hands. All these matters have been a drive for more research to come up with other possible measurement techniques.

2.1.5.3. Bisection method

The literature shows that much research have been conducted to find and study the best methods to assess distances. Bisection according to Da Silva [23] is also used to examine distances up to hundreds of meters. Humans naturally move and control their bodies accurately and with a high degree of proficiency, specifically, within personal and action space [95]. Therefore, the perceived space is a major key for any distance estimation technique. Gilinsky [37] performed experiments showing a great compression in distance reported using bisection. However, these results were not enough strong since only two subjects were involved. Bodenheimer et al. [38]; Da Silva, [23]; Purdy and Gibson [39]; Rieser, Ashmead, Talor, & Youngquist [40] conducted the same experiment but with hundreds of observers and showed that real world distances were precisely reported using bisection. Interesting results were reported by Lappin et al. [41] that demonstrated a considerable impact of the environment context on distance estimations. Estimations were different from the same experiment in two different environments.

2.2. Depth Perception in VR

Virtual Reality provides an environment to study perception research because different features of the world can be handled and controlled through the VR system. Depth perception experiments that cannot be done in the real world, in real time, will be able to be performed with the use of VR. This will allow one to study the elements influencing space and distance perception.

Many studies have shown a consistent underestimation of the judged distance in VR with HMDs [43,13]. VR environments suffer from several limitations. To benefit from VR systems to study depth perception, it is necessary to take into consideration these

limitations that are challenging to cope with and should be solved. Among the main limitations are the quality and size of HMD displays. The resolution content of most HMD displays is low, and the field of view is far narrowed as compared to human normal field of view. Additional limitations are involved in the distance underestimation issue, such as vergence-accommodation conflict and screen distance. Section 3.1 of this chapter presents the state-of-the-art review in virtual reality and depth perception. Section 3.2 examines previous work done in displaying real world content in VR.

2.2.1. Depth Perception in Virtual Reality

VR HMDs have a great potential to advance many fields, such as research, education, and training. However, their limitations must be addressed and improved before they can be fully applied in those areas. Many studies have been conducted to review and study the main issue in VR, depth perception, and more particularly distance misestimation [43,13,4]. Even after a decade, many other research issues in VR are still being actively investigated. Understanding the different visual information or physiological depth cues used by the brain to process and infer depth perception has been an active and ongoing research question for decades. Studying how these different depth cues interact and what are the contributing factors involved in spatial representation of physical objects in the world will help in understanding the information input processes. Understanding the interaction between the various depth cues will improve the comprehension of these basic issues and improve depth perception in these environments. Witmer and Sadowski [44] concluded that depth perception is the major problem that needs to be studied as it is the main virtual environment (VE) research question. Blind walking has been used as a method to measure and evaluate the differences in distance estimations made in the real world and

the virtual world. For that, the basic experimentation was to compare the same scene with the same objects in both environments. For that purpose, a VE scene of the same real-world scene was developed. Results showed a difference between distances reported in the real world and ones in the VE. As such, possible explanations related to binocular disparity and other depth cues have been proposed for further studies.

Several psychology studies on the neurological basis of depth perception have investigated the different mechanisms used in depth perception and how they interact and impact the way we perceive objects in the physical world. Howard et al. [43] studied the different visual attributes and qualities passed to the brain to determine depth perception of objects. The purpose of their work was two-fold. First, the contribution of each depth cue as a factor in depth perception was evaluated separately of others by inputting only one depth cue at a time. Second, the relationships between different depth cues and their contribution together in-depth perception accuracy were evaluated. The goal was to understand what are the depth cue relationships that impact depth perception, if incorporated together.

Research in human visual system depth perception has been a source of inspiration for research in depth perception in VEs. Jack Loomis and Joshua Knapp [13] examined egocentric distance perception (the distance from the observer to the object) in VR by comparing the performance of distance estimation between VEs and real-world environments. Different measurement mechanisms were employed to estimate depth perception and results have shown that there is a significant underestimation of distance perception in VE.

Loomis and Knapp [4] investigated how HMDs impacted the quality of depth perception in the virtual world in which visually directed triangulated walking [4] was used as a protocol to measure distance perception. The work examined the different factors leading to distance underestimation in HMDs, among them we find field of view of HMDs, problems related to the use of binocular stereo technique in HDMs, and vergence-accommodation conflicts. The work began by defining the distance estimation concept and the different zones of the distance values involved. They then studied the visual cues involved in each distance zone with a focus on experimenting with one distance estimation compared to estimations on the real world. To study, to what extent, the quality of an image affected the egocentric distance perception, different image configurations (i.e., different resolution and field of view) with the same stereotypical tiled texture maps, as the one in the real world, were tested. The study had an observer with normal or corrected vison view an object and then walk blind folded to the viewed object. A comparison was made between the distance of the observed objects as reported by the subjects in the real world and in the VE using high- and low-quality computer-generated images. A difference in the reported distances between the real environment and the virtual environment was reported, but surprisingly, in the virtual environment, little difference in distance was reported between high quality and low-quality images. The work concluded that the quality of computer-generated images has no impact on the depth perception in virtual environment. Thompson et al. [4] also showed that image quality does not influence distance perception.

Willemsen et al. [45] followed the work of Loomis and Knapp [4] and extended the experiments by trying to understand and validate the hypothesis that mechanical features of HMDs are the reasons behind the egocentric distance misestimation using VR HMDs.

A simulated HMD with the same conditions and configuration as a real HMD was developed. A comparison of distance estimations from 2 to 25m using direct and triangulated blind walking in both the VE, with a HMD, and the simulated HMD was performed. Results of experiments showed that using the simulated HMD made people feel like the environment and scene was compressed and they then underestimated the distance. This may explain why the HMDs influence distance perception.

Plumert et al. [19] conducted a study comparing depth perception in the real world and in VEs using both HDMs and large screen immersive displays. Three different experiments were performed to compare the accuracy of distance perception between the real and VE using distances between 20 and 120 ft. In the first experiment, participants measured the time it took to walk to objects in both the real and VE using a stopwatch. In the second experiment, participants estimated the time it would take to walk to an object with eyes covered and uncovered. The third experiment further evaluated the distance estimations in conditions with eyes covered and uncovered. A significant underestimation of distances was recorded in the three different experiments with head-mounted displays as compared to the virtual environments with large screen immersive displays.

Other research has been conducted to understand and explain this issue and the factors leading to depth misestimation. Knapp and Loomis [2] investigated the impact of the field of view on depth perception. Using blind walking and verbal reporting to get distance estimations measurements from observers under two different HMD configurations: 1) limited field of view, and 2) large field of view. Results showed that the field of view has no influence on the distance perceived by the observers. A similar research

question was the purpose of the work of Creem-Regehr et al. [16] in which experiments using HMD VRs with different field of views showed no impact on the distance perception.

In another study, a comparison of the performance with monocular viewing and binocular viewing was shown to have no impact on the distance misestimations using HMDs. Murgia et al. [14] and Foley et al. [46] examined the performance of object size estimations and object distance estimations and concluded that the two estimations are different but unconnected as the visual processing is done separately and not linked to the retina movements when eyes are trying to move to focus on an object.

In the last two years, research has been conducted to solve the depth perception issue with developing mechanical and technological solutions. Nitish et al. [26] believed that traditional optics are the main cause of near eye display problems and their inability to afford the required depth cues to get accurate depth perception. Two systems for near-eye displays were developed using focus tunable lenses and mobile gaze-tracking technology. The system concentrates on the focus cue by tracking the positions in the scene where the eyes are looking and updating the focus in real time. Reducing the vergence–accommodation conflict was also implemented as part of their contribution.

Research by Konrad and Kong [27] worked on a similar concept to reduce vergence accommodation conflict using tunable focus cues with the implementation of a defocus blur and focus cues to produce depth perception. Table 2.2 summarizes the main work done in depth perception issue in VR categorized depending on the protocol used to measure distance estimation accuracy.

Table 2. 2. Summary of the evaluation protocols used in VR.

Experimental and Estimation Protocol	Research Work
Triangulated walking task	Loomis and Knapp [13]
	Loomis and Knapp [4]
	Willemsen et al. [45]
Directed walking task	Creem-Regehr et al. [16]
	Jack Loomis and Joshua Knapp [13]
	Loomis and Knapp [4]
	Willemsen et al. [45]
	Plumert et al. [19]
	Jack Loomis and Joshua Knapp [13]
Blind walking	Knapp and Loomis [2]
	Witmer and Sadowski [44]
	Howard et al. [43]
	Jack Loomis and Joshua Knapp [13]
	Willemsen et al. [45]
	Plumert et al. [19]
Movement of object in the VE using a Joystick	Murgia and Sharkey [14]
Verbal reporting	Knapp and Loomis [2]
	Jack Loomis and Joshua Knapp [13]
	Plumert et al. [19]
	Nitish et al. [26]
	Konrad and Kong [27]
A model to predict the perception of location and the perception of the extent	Murgia et al. [14]
	Foley et al. [46]

2.2.2. Real-World VR content

Parallax is desired for stereoscopic panoramas where the scene is captured from different

view positions. Among the existing approaches for stereoscopic VR stitching are the ones

proposed by Couture et al. [59] and Zhang and Liu [60] where the idea is to stitch many FOV limited input images obtained from rotating a pair of stereo cameras [59]. These approaches produce limited depth, and they are mainly used for static scenes, which will make them difficult to use for VR stereoscopic video that needs live video for dynamic scenes. Hedman et al. [61] proposed a stereoscopic reconstruction of the scene before rendering it to the display. The captured images are reconstructed using textured 3D meshes that can then be rendered to a VR HMD. This method is still also not convenient for a real VR system because it is applicable only to static scenes and not dynamic ones. Real VR systems require displaying real-world video to VR HMDs, also described as real-world VR. A different approach has been widely used for earth observation from satellites.

The pushbroom imaging [62] method suggested by Gupta and Hartley where the camera model is designed as a pin-hole camera that moves along a linear trajectory in space. However, this approach is only used for static scenes and cannot be applied to dynamic scenes as required by real VR systems.

A suggestion to tackle these challenges was to rotate a camera around its optical center. Many previous studies proposed different alternatives to the same idea, and the main ones are [63, 64, 65]. A stereoscopic panorama is then generated by choosing suitable columns from the input views. The fundamental feature of these approaches is that the output stereo image is omnidirectional and result in reasonable depth in all viewpoints. Even though, the output image does not correspond to the viewpoint dependent output image, the generated depth is plausible according to Seitz [66]. These approaches that are based on viewpoint independent aspect are more practical for real time VR systems. According to Shum [67], they reduce considerably the computational cost and storage need

because of the use of a single pair of input views to produce stereoscopic depth. Recent research [68] has demonstrated that omnidirectional generated images can be achieved using fewer cameras, as few as three wide angle lenses (fisheye lens), however, this method produces an output image with low quality resolution.

The challenging issue in applying the above discussed methods is that the video output of dynamic scenes is difficult to generate in practice. The main cause of this limitation is the large number of input images processed by these approaches, required to acquire enough dense input strips of the scene, which makes acquiring dynamic data unfeasible.

In this thesis, we are presenting a different approach for improving distance estimations for real world VR content. An approach that employs a set up with only two cameras. Since the system requires only two cameras, it is less expensive than existing stereo real-world VR generation systems.

CHAPTER 3
DISTANCE ACCURACY OF REAL ENVIRONMENTS IN VIRTUAL REALITY HEAD-MOUNTED DISPLAYS

Distances are consistently underestimated in virtual environments (VEs), compared to the real world [70] [71]. The reason behind this underestimation is still not understood. Extensive research has been done to explore this question, but compared to virtual VR rendering, we find less research done in distance underestimation when real world scenes are displayed to HMDs. This first thesis goal is to investigate the type of systems referred to as real VR content. This chapter describes our system prototype developed for real VR content. Previous research used a computer-generated scene [60][65][67]. This work used a dual-camera video feed system through a Virtual Reality (VR) Head Mounted Display (HMD). We examined distance estimation in real environments rendered on HMDs. Two models were evaluated: a video-based and a photo-based. We used protocols (**see section 2.1.5**) already proven to accurately measure real-world distance estimations to compare distance judgment performance in the real world and these two evaluated VE models. The purpose is to explore whether the misjudgment of distances in using HMDs could be due to a lack of realism, or not.

3.1. Real VR Content: Motivation

Virtual reality can become a significant apparatus in real life tasks and activities. Virtual systems will be handy in dangerous and complex systems such as in firefighting, which

was the target environment behind this research. VR is now used in training systems in many different fields [13] [69]. In VR training systems, the distance underestimation may be tolerated since it is just for training purposes. However, this underestimation cannot be tolerated in safety critical purposes such as saving people's lives or medical surgeries. Typically, VR is used to display a model that was created somewhere else, but we feel there is great promise in using VR to display and render real world scenes. As an application, Firefighters use VR systems for training to immerse them in different scenarios, mimicking the possible situations they may face in real life. Firefighting and rescuing victims are extremely dangerous activities that put the life of the Firefighter in danger [69]. In this chapter we study the performance of distance accuracy in experiments with 18 participants and report on the differences of distance accuracy as reported by the observers.

This paper is organized as follows: section 3.2 discusses previous work on depth perception in VR; section 3.3 represents the material and method followed for the study; the procedure and elements of the study are presented; section 3.4 is the results and discussion of the output gotten from the experiments; the final section draws the conclusion and future work.

3.2.   Experimental Design and Setup

The purpose of this chapter is to study and compare distance estimations in VR headsets when a real scene is used instead of virtual scene. We ran an experiment to measure distance estimates using commonly used protocols in measuring real-world distances, blind walking, and verbal reporting, as discussed in related work [70] [71]. The studied distances are 2, 3, 5, 7, and 9m. Distances in the real-world seen by subjects was also studied and

used as a control condition to validate the results of distances judged using the HMD. Subjects estimated distances by looking at the real scene (video) through the HMD, and also by looking at a static image of the scene rendered to the HMD.

Figure 3. 1. Overview of the prototype.

The experiment used the Oculus Rift DK2 HMD, which has two 1920 x 1080 displays with a 90-degree field of view. The real scene was acquired and rendered in real time. We developed a prototype of the architecture that we are working with, presented in figure 3.1. Two cameras are used that are streaming live videos to the headset. The two cameras were positioned such as they acquire video as the human eye would (with respect to parallax).

First Experiment Model: Live Video Rendering (Real + HMD)

The first model uses a live video feed from two cameras to the HMD (shown in figure 3.1). For the study reported here, the two scenes acquired by the two cameras are then rendered

unto the two displays of the Oculus Rift. Most of the previous research studied a virtual replica of the real environment by creating a virtual model. These video streams retain the fine detail of the real scene. This approach did not require any additional elements to be added in order to keep realism in the environment.

Second Experiment Model: Photo Based Rendering (Photo + HMD)

For the second model. The right picture taken from the right camera (Microsoft LifeCam camera) is rendered to the right eye and the left picture from the camera (Microsoft LifeCam camera) is rendered to the left eye on the Oculus Rift. The left and right images rendered were done so such that the original parallax was retained. These static images retain the fine detail of the original photographic textures. This approach did not require any additional elements to be added to order to keep realism in the environment.

3.3.   Method and Design Procedure

The experiment was conducted in a university building (at UND). The hallway is a 2.28 × 30.4 meter hallway. Figure 3.2 shows the hallway and referent object (stool) setting used in the experiment. The experiment tested three environmental conditions: a real-world condition; a real-world condition with the HMD; and a real-world static photo condition. For each environment two protocols were used: blind walking and verbal reporting. The target object used was a stool.

For the blind walking protocol, the stool was placed at different distances and observers were asked to view the environment and the target location for few seconds until they were confident about their distance from the stool. Then, they closed their eyes and walked towards the stool. For the verbal reporting protocol, observers viewed the stool and

verbally reported the distance they perceived using whatever unit they were comfortable with. Eighteen subjects participated in the experiment and distances were randomized.

Figure 3. 2. The hallway and referent object (stool) setting used in experiment.

Variables and Design

Table 3.1 summarizes the different independent and dependent variables used in the study.

a) *Independent Variables*:

PARTICIPANTS: Eighteen students aged from 20 to 30 (undergraduate and graduate) participated in the experiment. Each participant spent an average of 2 hours performing the experiment.

ENVIRONMENT: Participants estimated distances of the target object in three different environments. In the real-world environment, subjects viewed the object, and did not look through the HMD. This condition is the control condition. In the real + HMD environment, subjects viewed the real-world object through the HMD. In the photo + HMD environment, subjects viewed the object as a static image through the HMD.

Table 3. 1. Dependent and independent variables for the experiment.

INDEPENDENT VARIABLES		
Participants	18	Random variable
Environment	3	Real world Real + HMD Photo + HMD
Protocol	2	blind walking verbal reporting
Distance	5	2, 3, 5, 7, 9 meters
DEPENDENT VARIABLES		
Judged distance	measured from each protocol, meters	
Error	judged distance – distance, meters	

PROTOCOL: Both protocols to measure distances, were used by all of the participants. In the blind walking protocol (real world environment), the participant is accompanied by the experimenter while walking so they do not deviate and hit the wall. When the participant stopped, the experimenter measured the walked distance and the participant is walked back to another room until the second distance trial is ready. They are then brought back to the starting location. In the blind walking protocol (real + HMD and Photo + HMD environment), the participant is looking at the object through the HMD. When ready, they take off the headset and walk towards the target object while blind folded. In the verbal reporting protocol (all 3 environments), participants viewed the target object for a period and verbally state the distance they perceive the object to be away from them. They use whatever unit of length (feet or meter) they are comfortable with.

b) *Dependent Variables:*

The main variable is the estimated distance walked or reported by the participant. The error variable is the second dependent variable; an error value less than 0 means

an underestimation of the distance, a value greater than 0 means an overestimation of distance, and close to 0 means an almost correct judgment of distance. A design of 18 (participant) × 3 (environments) × 2 (protocols) × 5 (distance) was used generating 540 data points.

3.4.   Results and Discussion

Experimental results are shown in Figures 3.3 and 3.4 where actual distance is plotted against estimated distance. In all figures, VRP is Verbal Reporting and BW is Blind Walking. Figures 3.3 and 3.4 show the results for the blind walking protocol and verbal reporting protocol, respectively, for the 3 environments. All of the results show an underestimation of distances in the VR environments (real + HMD and photo + HMD).

The three environment conditions evaluated: the real + HMD, the real + photo + HMD, and the real-world environment as the control condition. The estimations were measured using blind walking protocol. The black line refers to the veridical performance. A mean value close to the veridical line (the black line) means a better estimation of the distance. A mean value far from the veridical line means an underestimation of the distance. The closest we are to the veridical line, the better the estimation is.

We can classify the confidence of the estimated distance using percentages. Table 3.2 shows percentages of actual distance for each trial distance and the mean percentage of distance. Blind walking mean percentage accuracy in the real-world environment was 90%; in the real + HMD environment was 80% and the photo + HMD was 81%. Verbal reporting mean percentage accuracy in the real-world environment was 92.4%; in the real + HMD environment was 80.2% and the photo + HMD was 81.4%. Each row in the table 3.2 shows the estimation accuracy for each environment condition. Each column in that row shows the

Figure 3. 3. **The principal results plotted as the mean judged distance against the actual referent distance – blind walking protocol.**
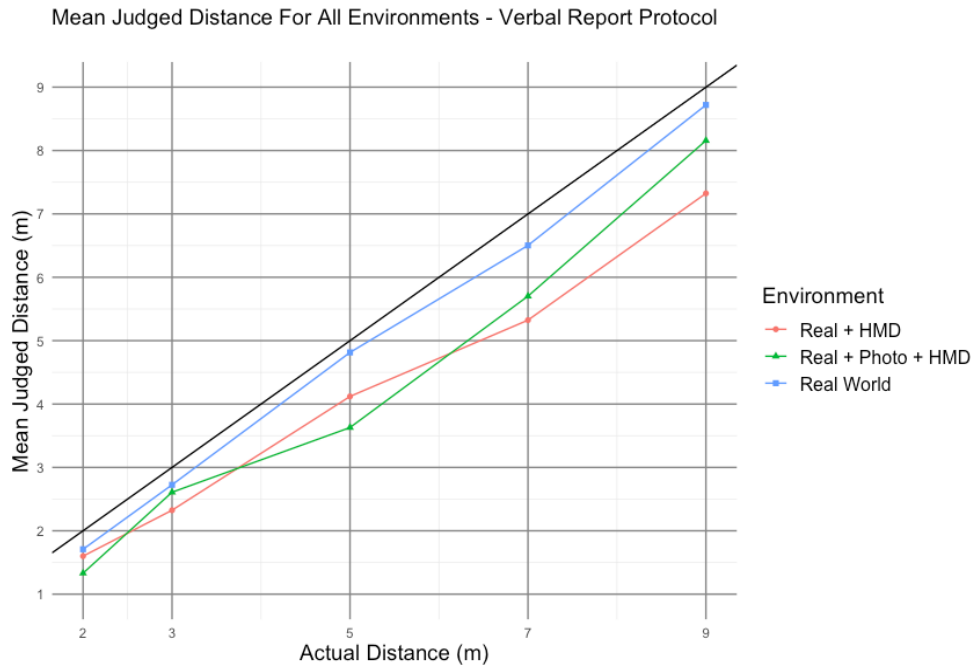
Figure 3. 4. **The principal results plotted as the mean judged distance against the actual referent distance - verbal report protocol.**

estimation accuracy for each distance trial. The bold values show the mean estimation accuracy for each environment condition.

Table 3. 2. Accuracy of judged distances as percentage of actual distance.

Distance		2	3	5	7	9	Mean
Blind Walking	Real World	98%	96%	87%	87%	82%	**90%**
	Real + HMD	95%	86%	80%	70%	69%	**80%**
	Photo + HMD	87%	93%	76%	71%	78%	**81%**
Verbal Report	Real World	85%	91%	96%	93%	97%	**92.4%**
	Real + HMD	67%	86%	84%	83%	81%	**80.2%**
	Photo + HMD	74%	77%	72%	93%	91%	**81.4%**

Accuracy in the blind walking decreased in the real + HMD environment compared to the control condition. Distances in the photo + HMD environment were only a little better than the real + HMD environment. Distances using the verbal reporting protocol gave almost the same results as the blind walking protocol. Noting that subjects using the verbal reporting protocol were closer in judging distances than the blind walking protocol by 2%. These results demonstrate a level of underestimation using HMDs of 81%, which is what was observed in the VE in the literature (underestimations of 42–85%).

As a visual aid, figures 3.5 and 3.6, show the results with the mean error (estimated distance – actual distance). For 2m and 3m distances, in all environments blind walking had less underestimation than verbal reporting. 5m, 7m and 9m distances had less underestimation in all real environments than the real + HMD environment. In all environments with blind walking the level of underestimation increased with increasing distances. However, for verbal reporting, the level of underestimations was variable among the different environments. Verbal reporting results are more variable than blind walking

Mean Error for Each Judged Distance - Verbal Report Protocol
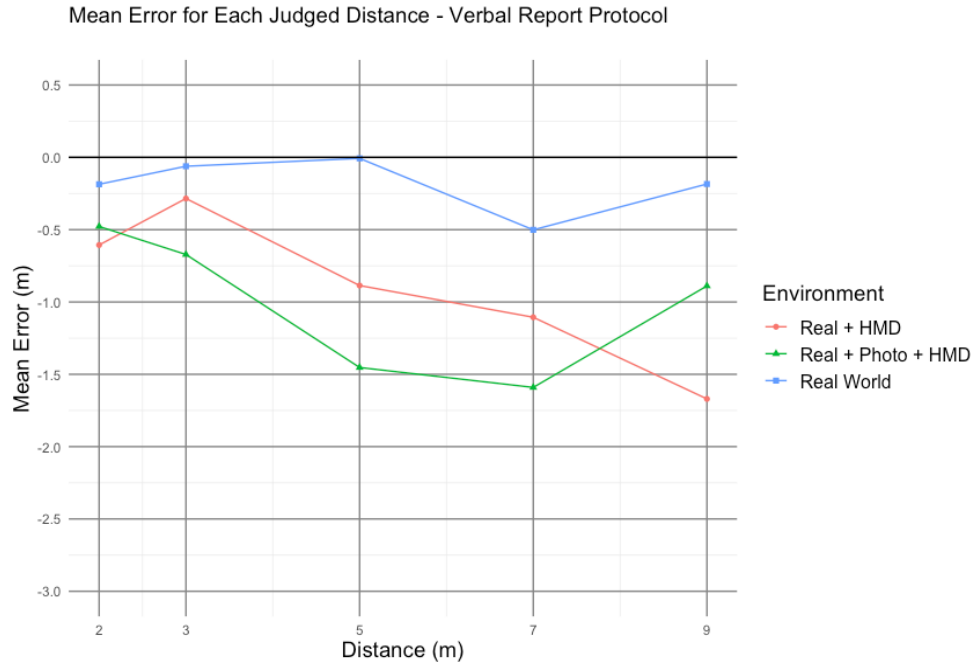
Figure 3. 5. Estimation errors - blind walking protocol.

Mean Error for Each Judged Distance - Blind Walking Protocol
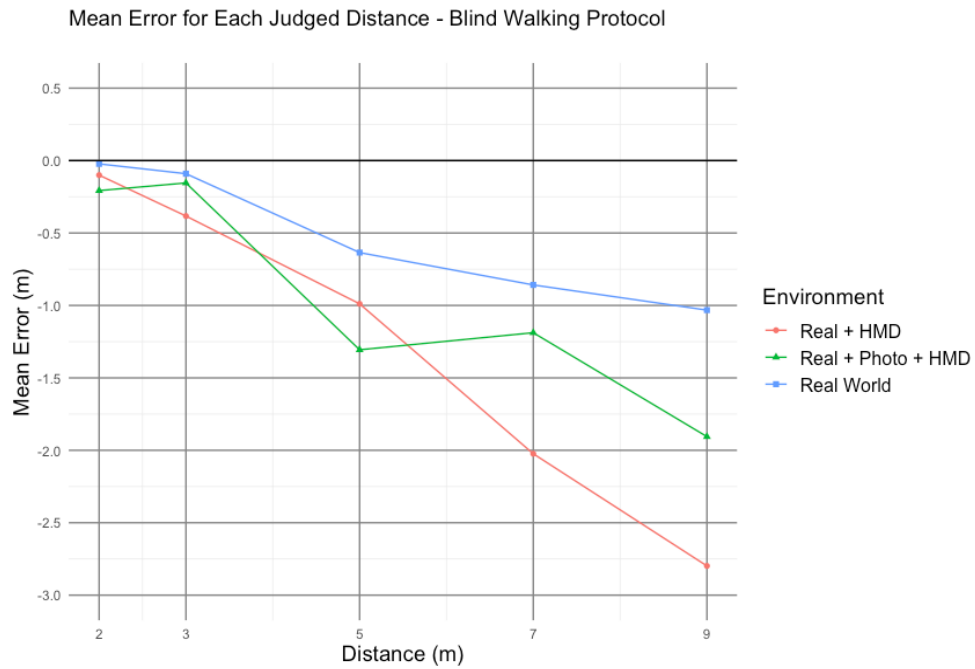
Figure 3. 6. Estimation errors - verbal reporting protocol.

results. The three environment conditions were assessed: the real + HMD, the real + photo + HMD, and the real-world environment as the control condition. Estimation errors are represented as the mean error for each judged distance. The mean error is calculated as the

(estimated distance – actual distance). The black line indicates the ideal performance (estimation error value of is 0) which is an accurate estimation of a distance. An error value less than 0 (below the horizontal black line) means an underestimation of the distance, a value greater than 0 (above the horizontal black line) means an overestimation of distance, and close to 0 (close the horizontal black line) means an almost correct judgment of distance. The closest we are to the horizontal black line, the better the estimation is.

For each participant, error estimations are reported in figure 3.8 for the blind walking protocol and figure 3.9 for the verbal reporting protocol. Figure 3.7 below explains the boxplots in figures 3.8 and figure 3.9.

Median

The median (middle quartile) marks the mid-point of the data and is shown by the line that divides the box into two parts. Half the distance estimations are greater than or equal to this value and half are less.

Inter-quartile range

The middle "box" represents the middle 50% of distance estimation values for the group.
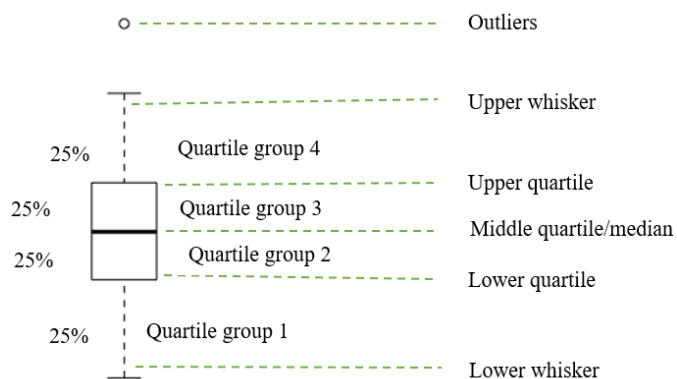
Figure 3. 7. Boxplot interpretation.

The range of distance estimation values from lower to upper quartile is referred to as the inter-quartile range. The middle 50% of distance estimation values fall within the inter-quartile range.

Upper quartile

Seventy-five percent of the distance estimation values fall below the upper quartile.

Lower quartile

Twenty-five percent of distance estimation values fall below the lower quartile.

Whiskers

The upper and lower whiskers represent distance estimation values outside the middle 50%. The minimum is shown at the far down of the chart, at the end of the bottom "whisker." The maximum shown at the far up of the box.

There is a consistent underestimation in the blind walking protocol as compared to the verbal reporting protocol. We notice in figure 3.8 how the estimation is highly variable among participants. Therefore, verbal reporting does not seem very reliable as a protocol for judging distances. Similar results were reported in previous AR & VR works. Total number of data points is 540. Total data points for each observer boxplot are 30. We can notice some outliers for most of the subjects. These subjects had one to two overestimations and very high underestimation errors. This shows some subjects had difficulties estimating some distances. However, the number of the outliers is insignificant compared to the size of the other estimations. For Verbal reporting protocol, we can notice some outliers for subjects 4, 5, 6, 7, 8, and 17. These subjects had one to two overestimations and very high underestimation errors. This shows some subjects had difficulties estimating some

distances. However, the number of the outliers is insignificant compared to the size of the other estimations.
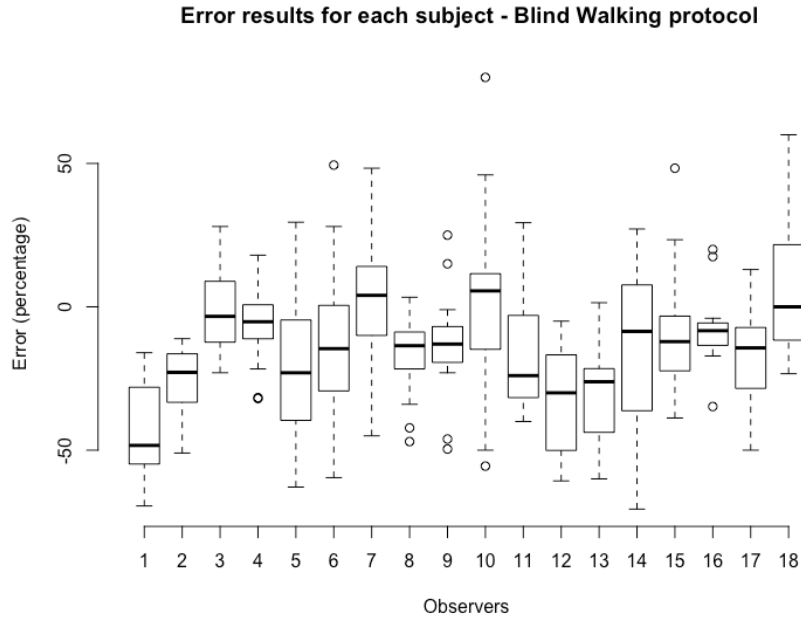
Figure 3. 8. The error results for each subject - blind walking protocol.
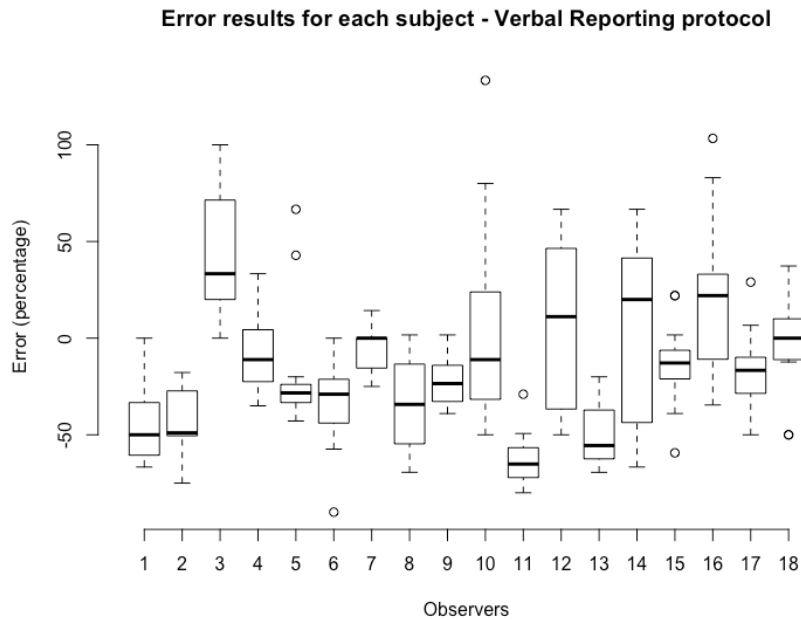
Figure 3. 9. The error results for each subject - verbal report protocol.

43

3.5. ANOVA Analysis

Analysis of variance (ANOVA) (shown in table 3.3) is used to describe and analyze the results. As shown, distances are underestimated in real scenes displayed in HMD, for both *real + HMD* and *photo + HMD* compared to the real environment (the control environment).

The F-Test of Overall Significance

From the ANOVA table results (table 4.3), the focus is on the F-statistic and the p-value of that F-statistic (which refers to the F- test overall statistical significance). The F-Test is used as a formal statistical test. If the overall F-test is significant, we can conclude that R-squared is not equal to zero and that the correlation between the variables is statistically significant.

The F value is used along with the p-value to decide whether the results are significant enough. If the calculated f value from the data in table 4.3 is larger (it is bigger than the F critical value found in a table [103]), it means something is significant, while a small p value calculated in table 4.3 means all the results are significant.

The 3 environments x 5 distances ANOVA showed a considerable disparity with the main effect being environment; Blind walking ($F(2,27) = 12.30$ and $p < 0.01$) and verbal reporting ($F(2,27) = 10.90$ and $p < 0.04$). (The F-statistic from literature is simply a ratio of two variances. Variances are a measure of dispersion, or how far the data are scattered from the mean. Larger values represent greater dispersion.) And (In statistics, the p-value is the probability of obtaining the observed results of a test, assuming that the null hypothesis is correct. A smaller p-value means that there is stronger evidence in favor of the alternative hypothesis.) Distances in the real world were easy to estimate, but the error increased with

increasing distance. However, for the *real + HMD* and *photo + HMD*, errors are inferred between distances which shows a difficulty in judging distances when using the HMD especially with the *photo + HMD* environment and with 3m, 5m and 7m distances (shown in figure 3.8). Distance judgment errors increased with increased distances for all environments $(F(2,51) = 3.73, F(2,51) = 10.13, F(2,51) = 12.9, F(2,51) = 17.02)$. However, there is no significant effect of environment for the 2m distance (shown in figure 3.8) $(F(2,51) = 0.81)$.

Table 3. 3. ANOVA results ANOVA results. The 3 environments x 5 distances ANOVA showed a considerable disparity with the main effect being environment.

Effect		N	n	d	F	p-value
Environment	All data	540	2	53	3.44	0.09
Environment	Blind walking	270	2	27	12.30	0.01
Environment	Verbal report	270	2	27	10.90	0.04
Environment	Blind walking, all environment, 2 meters	54	2	51	0.81	0.9
Environment	Blind walking, all environment, 3 meters	54	2	51	3.73	0.49
Environment	Blind walking, all environment, 5 meters	54	2	51	10.13	0.0001
Environment	Blind walking, all environment, 7 meters	54	2	51	12.9	0.03
Environment	Blind walking, all environment, 9 meters	54	2	51	17.02	0.04

In this chapter, we presented the first thesis contribution, the analysis of distance perception using two different methods to display real images from two cameras to an HMD. Consistent with the conclusions of previous work, we have found consistent distance compression in the HMD environments, even when displaying live video. VR has more potentials and challenges to tackle before one can use it in tasks and activities applicable to the real world. Our next step is to study and improve the different depth cues to enhance distance estimation in VR when using video. Other features of the system could also be

factors impacting distance compression and should be studied and understood in order to improve distance estimation in real environment rendering for VR. From the literature, the field of view FOV has been among the factors studied to understand its relationship with distance estimations. Our following goal is to study the impact of FOV on distance judgments in real environments displayed on HMDs (using the live video and the photo-based models). Our subjective experience with the photo-based model indicated it allowed for more depth sense than the video feed. Every video frame rendered from the two cameras looked much flatter than the similar photographs.

CHAPTER 4
EFFICIENT DISTANCE ACCURACY ESTIMATION OF REAL-WORLD ENVIRONMENTS IN VIRTUAL REALITY HEAD-MOUNTED DISPLAYS

This chapter expands on our previous research (described in chapter 3) that has been done to examine distance estimation of real environments rendered to Head Mounted Displays HMDs. Capturing and displaying real-world Virtual Reality (VR) content is still challenging and presents many undiscussed issues. Distance estimations is among the most challenging issues that are still investigated and not fully understood. In our initial work (described in chapter 3), we presented a dual-camera video feed system through a Virtual Reality Head Mounted Displays with two models; a video-based and a static photo-based model and we evaluated their distance estimations performance. The video-based (real + HMD) model and the static photo-based (real + photo + HMD) model averaged 80.2% of the actual distance, and 81.4% respectively compared to the Real-World estimations that averaged 92.4%.

This chapter presents the second thesis's contribution where we are investigating this underestimation and developing an improved model based on enhancing the field of view FOV of the displayed scenes to improve distance judgements when displaying Real-World VR content to HMDs. From our previous work, we concluded that the limited FOV is among the first potential causes of this underestimation, specially, the mismatch of FOV between the camera and the HMD field of views. Our proposed model is using a set of two

cameras to generate the video instead of hundreds of input cameras or tens of cameras mounted on a circular rig as previous works from the literature. The new developed approach was compared to the previous models from our previous work and showed an improvement of 11%, increasing the estimation accuracy from 80% to 91% and reducing the estimation error from 1.29% to 0.56%.

3.6.   Improving the Real VR Content Model

This work improves the performance of the real VR content model proposed in the previous work described in chapter 4 by improving the field of view mismatch between the HMD and the camera system. We are proposing a different and low-cost prototype involving only two cameras, which has not been done in previous works. We are presenting a real-world VR content system with a setup of two cameras that provides an extended field of view with high resolution and generates approximately a complete scene close to the two captured images. The two images from the two cameras must be translated to harmonious and coherent output image. Particularly, we are investigating one of the unanswered questions in previous works, whether the field of view mismatch between the camera and the HMD displays has an impact on the distance estimation performance. The narrow field of view of HMDs is among the biggest challenges in real-world VR research area. A second question this thesis chapter is trying to answer is to what extent a two-camera set up can provide an immersive real-world VR experience. Distance accuracy estimations in an experiment with 18 participants is performed using protocols already proven to accurately measure distance estimations (in Section 2.1.5). We compare this approach with the improved field of view with the previous three models we suggested in our previous work described in chapter 3. The results have demonstrated that the new developed approach

increased the previous results estimations by 11%. The estimation accuracy was improved from 80% to 91% based on mean absolute error calculations.

4.2. Methodology

In this chapter, we propose a real-world VR content image generation system. Two major stages are involved in the suggested framework comprising data acquisition and image generation components. The data acquisition component (described in section 4.2.1) is using two cameras to capture images for the stereo real-world content generation. The image generation component (described in section 4.2.2) has two steps; a camera calibration step (described in section 4.2.2.1) to enhance the camera input parameters and the stitching step (described in section 4.2.2.2) with feature extraction, feature matching, and image blending to stitch together the input images into one single image.

4.2.1. Data acquisition component for real time stereo generation

The proposed stereo data generation hardware prototype includes a camera model for stereo data generation. This camera model acquires video data and then passes it to the image generation component. The real time VR stereo scene is generated from stereo data where one image is generated for the left eye and another image is generated for the right eye. Many hardware-based methods have been suggested, but majority of these methods are expensive because they use many cameras. In this research, we propose a cost-effective hardware for creation of real time VR stereo image system. Our suggested approach includes only two cameras for capturing input image.

4.2.2. Real-time VR stereo generation component

This section describes the real-time VR stereo generation component along with its main sub-components. We are proposing a simple image stitching pipeline for real time VR

content, which is different from the previous suggested VR stereo image generation systems described in chapter 3. The whole VR stereo image generation component includes two sub-components, camera calibration and image stitching. The output of sub-component 1 is the input for sub-component 2.

4.2.2.1. Camera Calibration

The camera calibration process [72] involves mapping the camera coordinates to the world coordinate system. Two types of parameters are computed in this process: intrinsic and extrinsic parameters. The intrinsic parameters include the camera lens parameters, and extrinsic parameters include the camera orientation parameters. Each camera has both parameters approximately assigned in the beginning and then reprojection error and residual error are used to optimize these parameters. Three phases including feature extraction, feature matching, and computation of camera parameters are the main steps in the whole camera calibration process. The steps for the camera calibration are given in algorithm 1.

Feature Extraction

Feature extraction is a necessary first step in the camera calibration component where preselected features are extracted from the input images to be stitched. For the stitching process, we chose invariant features over traditional features because this method is vigorous for frames with differing directional information [73]. For these reasons, we chose as a feature descriptor Oriented FAST and Rotated BRIEF (ORB) for feature extraction [74]. According to the works by Jeon et al. [75] and Wang et al. [76], ORB speed computation is fast and effective in contrast to SIFT commonly employed for stereo panorama generation.

Algorithm 1 Camera Calibration Steps			
1	**Input**:	▷ Input Images	
2		*Img*	
3		▷ Initial camera parameters	
4		*ICP*	
5	**Output:**	▷ Computed camera parameters	
6		*CCP*	
7	**Steps**:		
8	**while** (Img)		
9		1: Extract consistent features	
10		£c ← **ORB** (Img_i , Img_{i+1})	
11		2: Feature matching	
12		Imf ← **RANSAC** (£c)	
13		3: Homography calculation	
14		Fmf ← **H** (Imf)	
15		4: Computing camera parameters	
16		CCP ← Φ(Fmf)	
17	**end while**		

Feature Matching

Feature matching is the second step in the camera calibration component. Features of contagious images are analyzed to eliminate mismatches and calculate the best matches. We chose Random Sample Consensus (RANSAC) algorithm for feature matching. RANSAC is an iterative method for estimating the transform matrix homography H that employs a set of random samples to detect matching relationships [77].

Camera Parameters Optimization

The optimization process of the camera parameters starts by initializing both the intrinsic and extrinsic parameters with random values from the input images. And then following an iterative process, the parameters are adjusted and optimized. The bundle adjustment approach is applied to find the most accurate matches between neighboring images, where at each iteration, images with the best matches are chosen for the next iteration.

Expressions of the intrinsic and extrinsic matrix parameters [78] are represented in equations 4.1 and 4.2.

$$M_{intr} = \begin{pmatrix} f_x & 0 & x_0 \\ 0 & f_y & y_0 \\ 0 & 0 & 1 \end{pmatrix} \tag{4.1}$$

$$M_{extr} = \begin{pmatrix} r_{11} & r_{12} & r_{13} | t_1 \\ r_{21} & r_{22} & r_{23} | t_2 \\ r_{31} & r_{32} & r_{33} | t_3 \end{pmatrix} \tag{4.2}$$

Equation 4.1 is the camera's intrinsic matrix, where f_x and f_y describe the focal length of x and y coordinates, x_0 and y_0 represent the principal point offset (the optical center). Equation 4.2 is the camera's extrinsic matrix that represents the camera's location in the world, and the direction it is pointing, where the rotation matrix r3x3 and the translation vector t3 x 1. The computational model for the camera using both matrixes can be written according to pinhole as (equation 4.3):

$$q_{cam} = sM_{intr} \, M_{extr} \, Q_{cam} \tag{4.3}$$

M_{intr} and M_{extr} are the set of intrinsic and extrinsic parameters, and s is the scaling factor value. Q_{cam} depicts the corresponding 3D points $(x_{cam}, y_{cam}, z_{cam}, 1)$ of each camera in real-world coordinates and q_{cam} depicts the 2D point $(m_{cam}, n_{cam}, 1)$ of the image surface. Hence, Equation (4.3) can be reformulated as (equation 4.4):

$$\begin{pmatrix} m_{cam} \\ n_{cam} \\ 1 \end{pmatrix} = sM_{intr} \, M_{extr} \begin{pmatrix} x_{cam} \\ y_{cam} \\ z_{cam} \\ 1 \end{pmatrix} \tag{4.4}$$

The mean reprojection error is used in each iteration to estimate the camera parameters. The reprojection error corresponds to the distance between the estimated projection points, $\hat{x}$, and the measured projection points, x. The reprojection error for parameter estimation can be written as (equation 4.5):

$$Error_{repro} = \sum_i d(x_i, \, \hat{x}_i)^2 + d(\acute{x}_i, \, \hat{x}_i)^2 \tag{4.5}$$

x_i and $\hat{x}_i$ denote the actual and estimated projection image points.

$\acute{x}_i$ and $\hat{\acute{x}}_i$ denote the imperfect and perfect images points.

d denotes the Euclidean distance between the image points (x_i , $\hat{x}_i$) and ($\acute{x}_i$, $\hat{\acute{x}}_i$).

The projection error is optimized iteratively to reduce the error and the camera parameters converge.

4.2.2.2. Image Stitching

The image stitching process consist of two main stages. The first stage involves the registration of the two images and matching the detected features to identify the superposed regions. In the second stage, the optimized parameters generated from the camera calibration process are used to stitch the images. As a final stage, a blending phase is done to remove the noticeable seams at the edges of the stitched images. The steps for image stitching process are given in algorithm 2.

Algorithm 2 Image Stitching Steps
1   **Input**:   ▷ Input Images
2   *Img*
3   ▷ Computed camera parameters
4   *CCP*
5   **Output:**   ▷ The Output image
6   I^p
7   **Steps**:
8   **while** (Img)
9   1: Image wrapping
10               $W_i \leftarrow \coprod_f(Img_i , Img_{i+1}, CCP)$
11   2: Image blending
12              $I_{blend} \leftarrow$ **Multi-Band** $(W_{i,}, W_{i+1})$
13   3: Panorama straightening
14              $I^p \leftarrow \boldsymbol{P_{strai}} (I_{blend(i)}, I_{blend(i+1)})$
15   **end while**

Image Alignment

Image stitching involves merging multiple images with different degrees of overlap to produce a high-resolution image. To generate results with seamless artifacts, most image stitching approaches need precise overlap and congruent exposures between images. The first phase in this process is the alignment of the contiguous images based on the corresponding features. The image alignment starts with the calculation of the displacement, *d*, between contiguous images, for example *I1* and *I2*. Then, the homography, H (3 × 3 matrix), is computed based on the displacement, *d*, and used to map the image plane of *I1* to *I2*. Wrapping image *I1* to the image plane of *I2* by applying the homography H is the last step in the image alignment process. The correlation between the two images I1 and I2 is described in equation 4.6:

$$I1 = H \times I2 \qquad (4.6)$$

Where H is a (3 × 3) matrix as shown in equation 4.7:

$$H = \begin{pmatrix} h_{11} & h_{12} & h_{13} \\ h_{21} & h_{22} & h_{23} \\ h_{31} & h_{32} & h_{33} \end{pmatrix} \qquad (4.7)$$

Image Blending

Image blending is the last step performed to eliminate the visible blurring and seams generated during the image stitching process. Many image blending techniques exist, such as Pyramid Blending [79], Alpha Blending [80], Poisson Blending [81], and multi-band blending [82]. The multi-band blending is chosen here as an image blending technique because of the effective results showed in the work done by Burt et al. [83].

The official SDK and Oculus Rift in Action book were used as a base to implement the package. The Appendices A, B, and C show examples of the code implementation.

The figures below show a comparison of the generated images on the Oculus. Figure 4.1 shows the comparison between the two models Real + HMD and Real + HMD + FOV and how much parallax (the difference between the two images) is rendered to the two Oculus eyes.

The two cameras are placed and separated by the same distance as human eyes. Figure 4.1 shows the rendered images captured from the different camera's viewing positions. The two images represented from the two cameras are the same with a slight difference, and the red lines are drawn vertically to point to that slight difference between the two images rendered to the oculus eyes. The horizontal yellow line is drawn to indicate the amount of displacement in the image position captured by the two different cameras. The image on the left shows no yellow line which means no displacement, and the image on the right shows a yellow line that points to the amount of displacement.
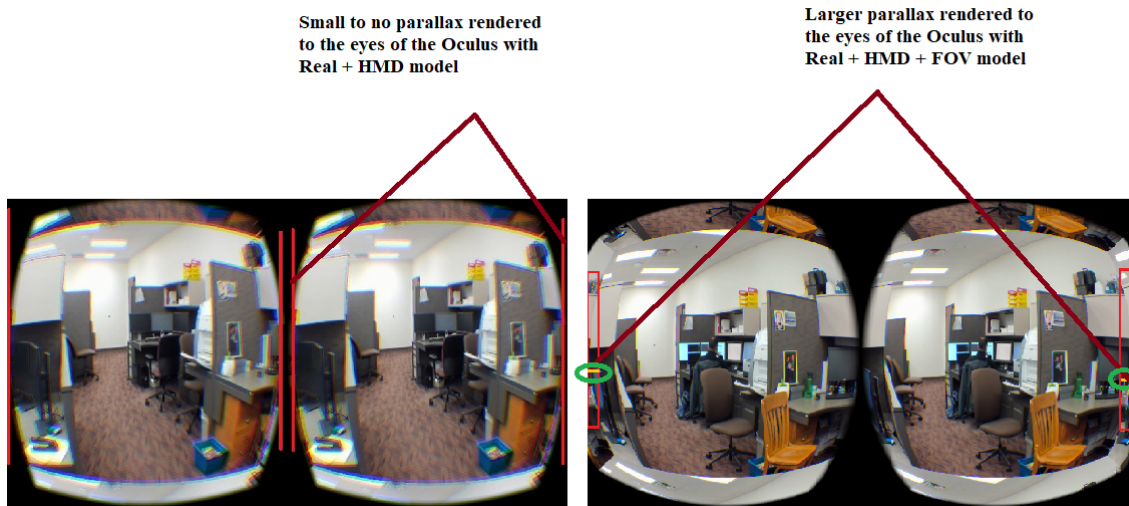
Figure 4. 1. Comparison of the Oculus view of the two rendered images on the two Oculus eyes for both models, the Real + HMD and the Real + HMD + FOV models.

Figures 4.2 and 4.3 show the results from the proposed system in chapter 3 (real + HMD model). The rendered images have little to no parallax on the generated images (figure 4.2). Figures 4.4, 4.5, and 4.6 show the results generated by the proposed model in

this chapter (Real + HMD + FOV model). The red line with the yellow line (drawn in figure 4.5) shows the parallax rendered on the display. There is more parallax rendered compared to the previous model (figure 4.2).

Figure 4. 2. The Oculus view of the two rendered images on the two Oculus eyes.

Left Eye   Left and Right Eyes   Right Eye

Figure 4. 3. The Oculus view of the left and right eyes.

Figure 4. 4. The Oculus view of the two rendered images on the two Oculus eyes.

Figure 4. 5. The Oculus view of the two rendered images on the two Oculus eyes - the red box shows the parallax which is more compared to figure 4.1.

4.3.   Material and Method

4.3.1. Experimental Design and Setup

The purpose of this work is twofold: firstly, to study and compare distance estimations in VR headsets when a real scene is used instead of a virtual scene; and secondly, to investigate the impact of the mismatch of the FOV between the VR displays and the camera system on distance estimations performance and whether improving the FOV will improve distance estimations performance or not. We are running an experiment to measure distance estimates using commonly used protocols in measuring real-world distances, blind walking, and verbal reporting, as discussed in related work [10] [71]. The studied distance is from 2 to 9 meters. Distances in the real-world seen by subjects were also studied and used as a control condition to validate the results of distances judged using the HMD. Subjects estimated distances by looking at the real scene (video) through the HMD, and by looking at a static image of the scene rendered to the HMD. The experiment used the

Figure 4. 6. The results generated by the proposed model (Real + HMD + FOV model). The Oculus view of the left and right eyes - the right image is on the right and the left image is on the left, the image on the center is the generated image on the display Oculus. The red line with the yellow line shows the parallax rendered on the display. There is more parallax rendered compared to the previous model.

Oculus Rift DK2 HMD, which has two 1920 x 1080 displays with a 90-degree field of view. The real scene was acquired and rendered in real-time. We developed a prototype (Figure 3.1 in section 3.2.1) of the architecture that we are working with. Two cameras are used (The figure shows only one camera) that are streaming live videos to the headset. The two cameras were positioned such as they acquire video as the human eye would (with respect to parallax).

We are comparing distance estimations performance between the two models from the previous work (Live Video Rendering (Real +HMD) and Photo-Based Rendering (Real + Photo + HMD)) and the new developed approach in this work in section 3 (Real + HMD + FOV). The goal is to investigate how improving FOV will improve distance estimation judgments.

First Experiment Model: Live Video Rendering (Real +HMD) The first model uses a live video feed from two cameras to the HMD (shown in figure 3.1). For the study reported here, we created a real replica environment by taking the two scenes acquired by the two cameras and rendered them unto the two displays of the Oculus Rift. To the knowledge of authors, this has not been studied before. Most of the previous research studied a virtual

replica of the real environment by creating a virtual model. These video streams retain the fine detail of the real scene. This approach did not require any additional elements to be added to keep realism in the environment.

Second Experiment Model: Photo-Based Rendering (Photo + HMD), For the second model, texture maps were created from single frames of the video used in the first model. The right picture taken from the camera is rendered to the right eye and the left picture from the camera is rendered to the left eye on the Oculus Rift. The left and right images rendered were done so such that the original parallax was retained. These static images contain the fine detail of the original photographic textures. This approach did not require any additional elements to be added to keep realism in the environment.

Third Experiment Model: Live Video Rendering (Real +HMD + FOV), the same model as the first one (Real + HMD) with the improved FOV approach described **in section 4.2.**

4.3.2. Method and design procedure

The experiment was conducted in a university building. The hallway is a 2.28 x 30.4-meter hallway (figure 3.2). The experiment tested four environmental conditions: a real-world condition; a real-world condition with the HMD; a real-world static photo condition; and a real-world condition with the HMD and the improved FOV approach. For each environment, two protocols were used: blind walking and verbal reporting. The target object used was a stool. For the blind walking protocol, the stool was placed at different distances and observers were asked to view the environment and the target location for few seconds until they were confident about their distance from the stool. Then, they closed their eyes and walked towards the stool. For the verbal reporting protocol, observers viewed the stool and verbally reported the distance they perceived using whatever unit they

were comfortable with. Eighteen subjects participated in the experiment and distances were randomized.

1. ***Variables and Design:*** Table 4.1 summarizes the different independent and dependent variables used in the study.

    a) *Independent variables:*

PARTICIPANTS: Eighteen participants got involved in the experiment, most of them are students at the university (undergraduate and graduate) aged from 20 to 30. Subjects spent an average of 3 hours performing the experiment.

ENVIRONMENT: Participants estimated distances of the target object in four different environments. In the real-world environment, subjects viewed the object and did not look through the HMD. This condition is the control condition. In the real + HMD environment and the real + HMD + FOV, subjects viewed the real-world object through the HMD. In the photo + HMD environment, subjects viewed the object as a static image through the HMD.

Table 4. 1. Dependent and independent variables for the experiment.

INDEPENDENT VARIABLES		
Participants	18	Random variable
Environment	4	Real world Real + HMD Photo + HMD Real + HMD + FOV
Protocol	2	blind walking verbal reporting
Distance	5	2, 3, 5, 7, 9 meters
DEPENDENT VARIABLES		
Judged distance	measured from each protocol, meters	
Error	judged distance – distance, meters	

PROTOCOL: Both protocols to measure distances, were used by all participants. In the blind walking protocol (real-world environment), the participant is accompanied by the experimenter while walking so they do not deviate and hit the wall. When the participant stopped, the experimenter measured the walked distance, and the participant is walked back to another room until the second distance trial is ready. They are then brought back to the starting location. In the blind walking protocol (real + HMD, Photo + HMD environment, and real + HMD + FOV), the participant is looking at the object through the HMD. When ready, they take off the headset and walk towards the target object while blindfolded. In the verbal reporting protocol (all 4 environments), participants viewed the target object for a period and verbally state the distance they perceive the object to be away from them. They use whatever unit they are comfortable with.

b) Dependent Variables:

The main variable is the estimated distance walked or reported by the participant. The error variable is the second dependent variable; an error value less than 0 means an underestimation of the distance, a value greater than 0 means an overestimation of distance, and close to 0 means an almost correct judgment of distance. A design of 18 (participant) x 4 (environments) x 2 (protocols) x 5 (distance) was used generating 720 data points.

4.3.3. Results and Discussion

Experimental results are shown in Figures 4.7 and 4.8 where actual distance is plotted against estimated distance. In all figures, VRP is Verbal Reporting and BW is Blind Walking. Figures 4.7 and 4.8 show the results for the blind walking protocol and verbal reporting protocol, respectively, for the 4 environments. The four environment conditions evaluated: the real + HMD + FOV, the real + HMD, the real + photo + HMD, and the real-

Figure 4. 7. The principal results plotted as the mean judged distance against the actual referent distance - blind walking protocol.
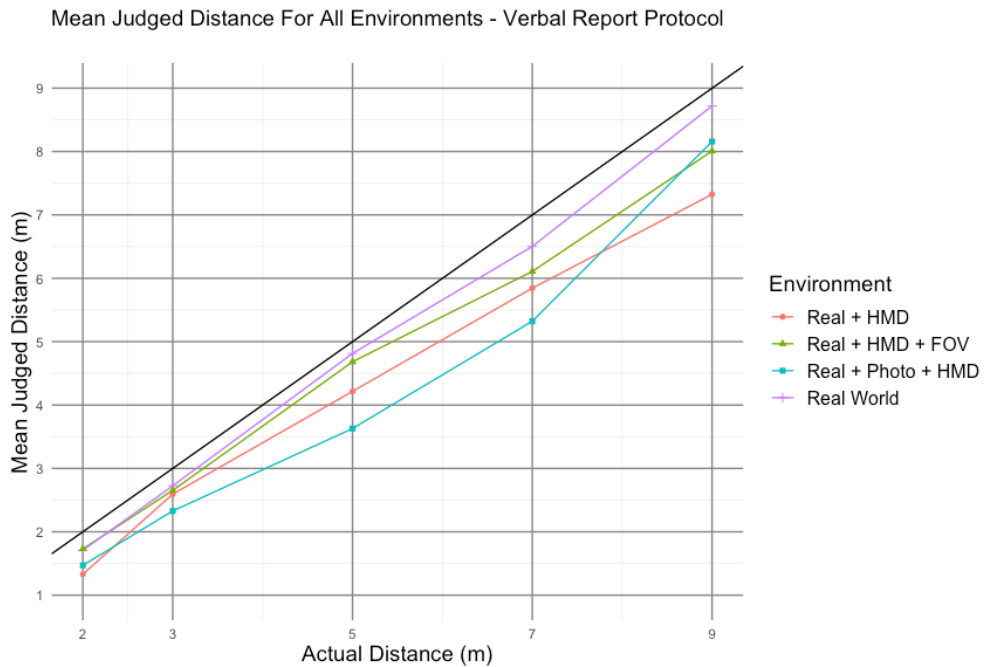
Figure 4. 8. The principal results plotted as the mean judged distance against the actual referent distance - verbal report protocol.

world environment as the control condition. The estimations were measured using blind walking protocol. The black line refers to the veridical performance. A mean value close to the veridical line (the black line) means a better estimation of the distance. A mean value far from the veridical line means an underestimation of the distance. The closest we are to the veridical line, the better the estimation is.

From our previous work, all the results showed an underestimation of distances in the two VR model environments (real + HMD and photo + HMD). However, we can see that the proposed VR environment in this work (Real + HMD + FOV) is giving promising results compared to the real + HMD environment and photo + HMD environment. For the blind walking results with the proposed approach, all distance estimations were improved compared to the real + HMD and real + photo + HMD. For the 2m distance, there is an overestimation of 10%. The mean judged distance for the 3m and 5m distances performed better than the control condition real world, with 3m at a mean of a 100% accuracy. The two distances 7m and 9m performed less than the control condition, the real-world environment, but better than the two previous VR models. Overall, the new developed approach performed better than the previous two models developed in the previous work. These results prove that the mismatch between the FOV of the VR displays and the cameras systems and the restricted FOV of the VR displays has a great impact on distance estimations of real VR content. Thus, improving the FOV improves dramatically distance estimations in the real VR content.

We can classify the confidence of the estimated distance using percentages. Table 4.2 shows percentages of actual distance for each trial distance and the mean percentage of distance. Each column in that row shows the estimation accuracy for each distance trial.

The bold italic values show the environment condition where the mean estimation accuracy performed better. Blind walking mean percentage accuracy in the real-world environment was 90%; in the real + HMD environment was 80% and the photo + HMD was 81%.

Verbal reporting mean percentage accuracy in the real-world environment was 92.4%; in the real + HMD environment was 80.2% and the photo + HMD was 81.4%. Accuracy in the blind walking decreased in the real + HMD environment compared to the control condition. Distances in the photo + HMD environment were only a little better than the real + HMD environment. For the new approach developed for the new environment Real + HMD + FOV, Blind walking mean percentage accuracy was 91%, and verbal reporting mean percentage accuracy was 87%. The new approach with the improved FOV performed better than the previous developed models with 11% improvement compared to the real + HMD and 10% compared to the real + photo environment, an average of 10.5% improvement compared to the two previous model.

Table 4. 2. Accuracy of judged distances as percentage of actual distance. Each row shows the estimation accuracy for each environment condition.

Distance		2	3	5	7	9	Mean	std
Blind Walking	Real World	98%	96%	87%	87%	82%	**89.97%**	**2.17**
	Real + HMD	95%	86%	80%	70%	69%	**80.2%**	**2.11**
	Photo + HMD	87%	93%	76%	71%	78%	**80.96%**	**2.17**
	Real + HMD + FOV	98%	100%	93%	83%	83%	*91.33%*	*2.16*
Verbal Report	Real World	85%	91%	96%	93%	97%	**92.46%**	**3.25**
	Real + HMD	67%	86%	84%	83%	81%	**80.43%**	**3.10**
	Photo + HMD	74%	77%	72%	93%	91%	**81.22%**	**3.46**
	Real + HMD+FOV	100%	100%	74%	88%	72%	*86.58%*	*2.08*

While we report the standard deviation std here, a more throughout analysis is presented in section 4.1.4 using ANOVA analysis. These results show how FOV mismatch impacts the distances assessment. Improving the FOV with the suggested approach in section 4.2 improved the performance with 10.5% compared to the previous models.

Distances using the verbal reporting protocol gave almost the same results as the blind walking protocol. Noting that subjects using the verbal reporting protocol were closer in judging distances than the blind walking protocol by 2%. These results demonstrate two important findings:

- a level of underestimation using HMDs of 81%, which is what was observed in the VE in the literature (underestimations of 42–85%).

- an improvement of distance estimations for the real VR content by 11% using the new developed stitching pipeline approach. A result that outperformed the last presented works from the literature.

As a visual aid, figures 4.9 and 4.10, show the results with the mean error (estimated distance – actual distance). The four environment conditions were assessed: the real + HMD + FOV, the real + HMD, the real + photo + HMD, and the real-world environment as the control condition. Estimation errors are represented as the mean error for each judged distance. The mean error is calculated as the (estimated distance – actual distance). The black line indicates the ideal performance (estimation error value of is 0) which is an accurate estimation of a distance. An error value less than 0 (below the horizontal black line) means an underestimation of the distance, a value greater than 0 (above the horizontal black line) means an overestimation of distance, and close to 0 (close the horizontal black

line) means an almost correct judgment of distance. The closest we are to the horizontal black line, the better the estimation is.

Mean Error for Each Judged Distance - Blind Walking Protocol

Figure 4. 9. Estimation errors - blind walking protocol.

Mean Error for Each Judged Distance - Verbal Report Protocol
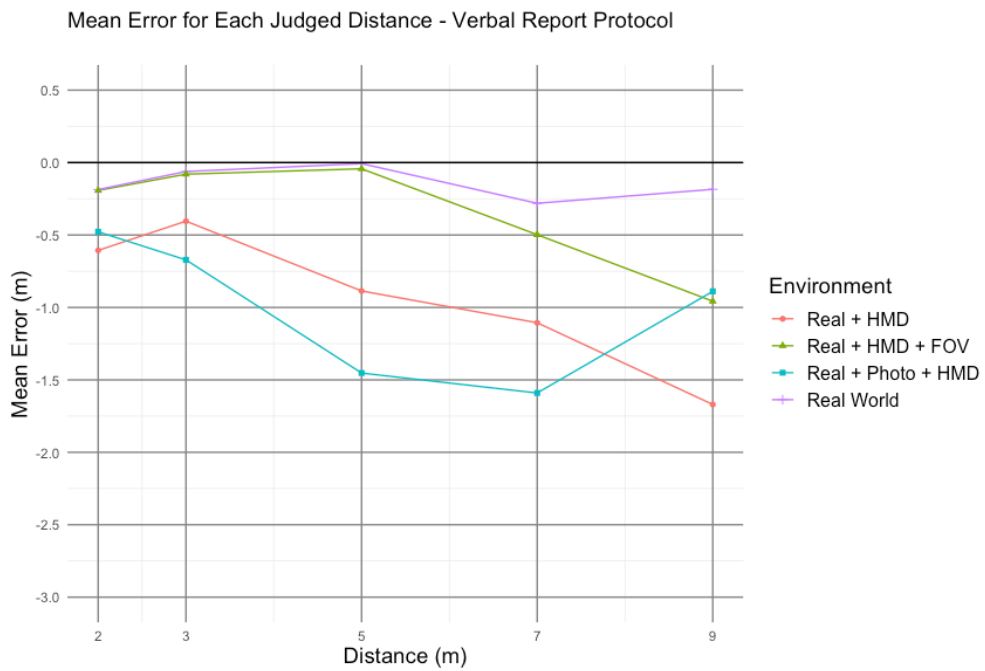
Figure 4. 10. Estimation errors - verbal report protocol.

From previous work results, 2m and 3m distances, in all environments, blind walking, had less underestimation than verbal reporting. 5m, 7m, and 9m distances had less underestimation in all real environments than the real + HMD environment. In all environments with blind walking the level of underestimation increased with increasing distances. However, the new approach results with real +HMD+ FOV environment has less underestimation compared to the previous two environments with all trial distances. The new evolved approach Real + HMD + FOV reduced estimation error from 1.29% to 0.56% compared to the previous developed approaches real + HMD and real + Photo HMD, showing an improvement for distance estimations of 11%. 3m distance has a mean error of 0 with a mean accuracy of 100%. 5m, 7m, and 9m distances in real + HMD + FOV environment had less underestimation than the three other environments with a smaller mean error, which shows the new approach ability to improve the accuracy of distances judgments. The 2m distance showed though an overestimation of 10%. For verbal reporting, the level of underestimation was variable among the different environments. Verbal reporting results are more variable than blind walking results.

For each participant, error estimations are reported in figure 4.11 for the blind walking protocol and figure 4.12 for the verbal reporting protocol. The boxplot interpretation is described in figure 3.7. Total number of data points is 720. Total data points for each observer boxplot are 40. We can notice some outliers for most of the subjects. These subjects had one to two overestimations and very high underestimation errors. This shows some subjects had difficulties estimating some distances. However, the number of the outliers is insignificant compared to the size of the other estimations.
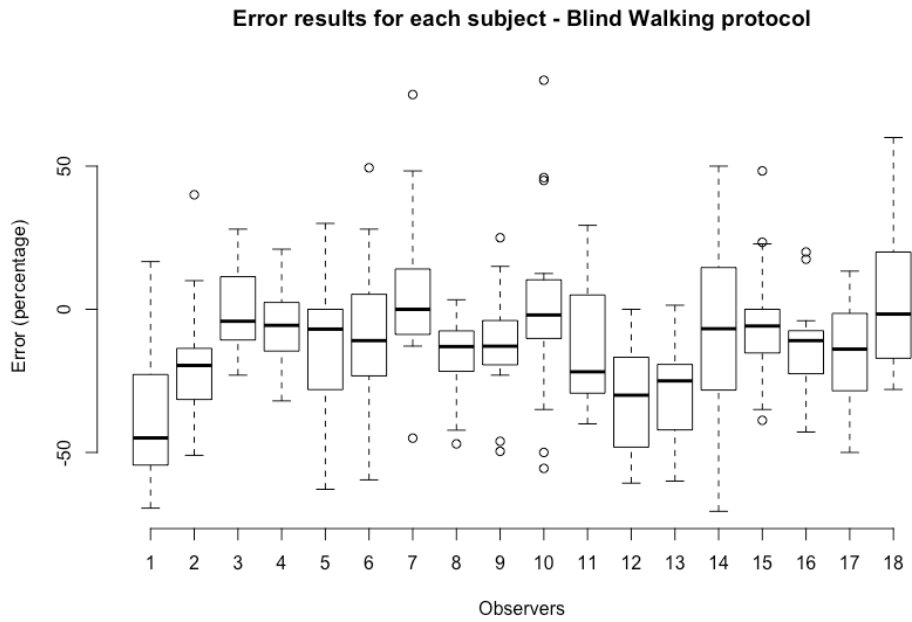
Figure 4. 11. The error results for each subject - blind walking protocol.
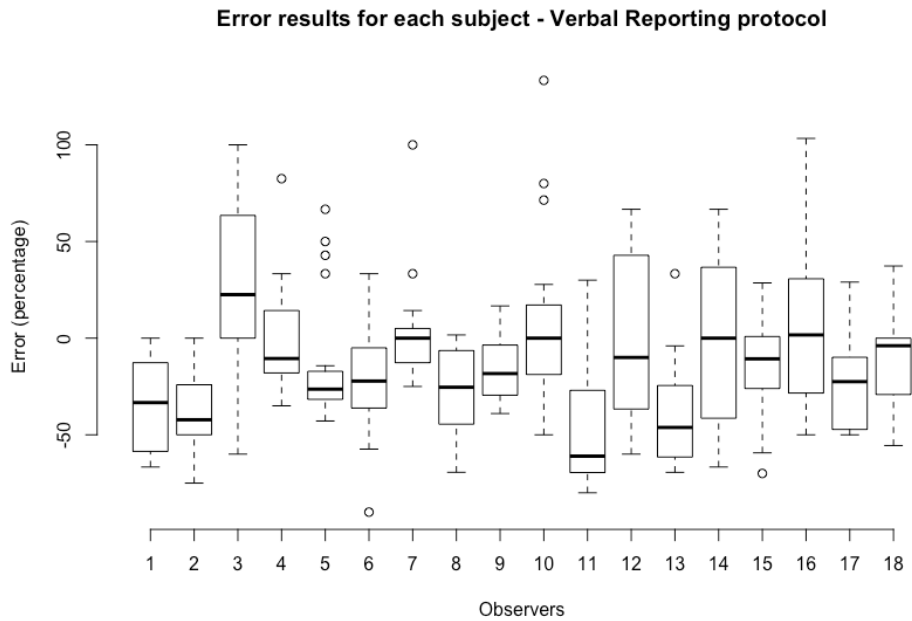
Figure 4. 12. The error results for each subject - verbal report protocol.

There is a consistent underestimation in the blind walking protocol as compared to the verbal reporting protocol. We notice in figure 4.12 how the estimation is highly variable among participants. Therefore, verbal reporting does not seem very reliable as a protocol for judging distances.

4.3.4. ANOVA analysis

Analysis of variance (ANOVA) (shown in table 4.3) is used to describe and analyze the results. As shown, distances are underestimated in real scenes displayed in HMD, for both real + HMD and photo + HMD compared to the real environment (the control environment). However, the new environment Real + HMD + FOV demonstrated a significant improvement of distance estimations compared to both real + HMD and photo + HMD.

The F-Test of Overall Significance

From the ANOVA table results (table 4.3), the focus is on the F-statistic and the p-value of that F-statistic (which refers to the F- test overall statistical significance). The F-Test is used as a formal statistical test. If the overall F-test is significant, we can conclude that R-squared is not equal to zero and that the correlation between the variables is statistically significant.

The F value is used along with the p-value to decide whether the results are significant enough. If the calculated f value from the data in table 4.3 is larger (it is bigger than the F critical value found in a table [103]), it means something is significant, while a small p value calculated in table 4.3 means all the results are significant.

The 4 environments x 5 distances ANOVA showed a considerable disparity with the main effect being environment; Blind walking ($F_{(3,356)} = 2$ and $p < 0.11$) and verbal

reporting (F(3, 356) = 1.55 and p < 0.19). (The F-statistic from literature is simply a ratio of two variances. Variances are a measure of dispersion, or how far the data are scattered from the mean. Larger values represent greater dispersion. And in statistics, the p-value is the probability of obtaining the observed results of a test, assuming that the null hypothesis is correct. A smaller p-value means that there is stronger evidence in favor of the alternative hypothesis).

Distances in the real world were easy to estimate, but the error increased with increasing distance. Same pattern for the real + HMD + FOV environment where distances were approximately following a similar behavior but were less accurate than the real-world environment. However, for the real + HMD and photo + HMD, errors are inferred between distances which shows the difficulty in judging distances when using the HMD especially with the photo + HMD environment and with 3m, 5m, and 7m distances (figure 4.12). Distance judgment errors increased with increased distances for all environments (F(3,68) = 7.14, F(3,68) = 5.85, F(3,68) = 7.35, F(3,68) = 3.26). However, there is no significant effect of environment for the 2m distance (figure 6) (F(3,68) = 2.57).

Table 4. 3. ANOVA results. The 4 environments x 5 distances ANOVA showed a considerable disparity with the main effect being environment.

Effect		N	n	d	F	p-value
Environment	All data	720	3	716	2.93	0.05
Environment	Blind walking	360	3	356	2	0.09
Environment	Verbal report	360	3	356	1.55	0.19
Environment	Blind walking, all environment, 2 meters	72	3	68	2.57	0.06
Environment	Blind walking, all environment, 3 meters	72	3	68	7.14	0.03
Environment	Blind walking, all environment, 5 meters	72	3	68	5.85	0.04
Environment	Blind walking, all environment, 7 meters	72	3	68	7.35	0.0002
Environment	Blind walking, all environment, 9 meters	72	3	68	3.26	0.02

CHAPTER 5
CONCLUSION AND FUTURE WORK

The work in this thesis is far from exhaustive and provides a strong foundation for further research in real VR content. This thesis goal was to improves distance estimations of real environments displayed in VR HMDs. This work was directed toward a twofold aim: Examining distance estimations when real content is displayed in HMDs instead of virtual content and improve distance estimations accuracy for real VR content. We examined distance estimation in real environments rendered to Head-Mounted Displays, where distance estimation is among the most challenging issues that are still investigated and not fully understood.

As many advancements have been made recently to deploy, and use, VR technology in virtual environments, it is still less mature to be used to render real environments. The current VR systems settings, which are developed for virtual environments rendering, fail to adequately address the challenges of capturing and displaying real-world VR content that these systems entail. Before these systems can be used in real life settings, their performance needs to be investigated, more specifically, depth perception and how distances to objects in the rendered scenes are perceived.

This thesis presented two main contributions that gives a strong basis to further scientific research in VR content. The first contribution introduced a dual-camera video feed system through a Virtual Reality Head Mounted Display. Distance estimations in real

environments rendered to HMDs were examined. Two models were evaluated: a video-based and a photo-based. An experiment with 18 participants was run to measure distance estimates using commonly used protocols in measuring real-world distances, blind walking, and verbal reporting. Real-world distances were compared to the two evaluated VE models. The purpose was to explore whether the misjudgment of distances in HMDs could be due to a lack of realism or not, with the use of a real-world scene rendering system. We found consistent distance compression in the HMD environments, even when displaying live video. We also found that when the model was rendered as static photo-based, the under estimation was less compared with the live video feed rendering. The real HMD model estimation accuracy averaged 80.2% of the actual distance, the real photo-based model averaged 81.4%, and the real-world estimations averaged 92.4% (which is the better accuracy). Additionally, our subjective experience with the photo-based model indicated it allowed for more depth sense than the video feed. Every video frame rendered from the two cameras looked much flatter than the similar photographs. We found that by controlling/adjusting the parallax between the two photographs we obtained greater accuracy in depth perception. However, we did not find a similar effect when using a video feed. The static feature of the two images allowed for more accurate processing and correction of the image's parallax before rendering them. However, for the video processing, the dynamic property made it difficult to control, in real time, the parallax of each frame. Therefore, there is a need for other alternatives for video rendering for VR content. This was the motivation and second contribution of this thesis.

The second contribution of this work expanded on the previous research model. The purpose was to improve the performance of the real VR content model in the first

contribution by improving the field of view mismatch between the HMD and the camera system. We proposed a different and low-cost prototype involving only two cameras. Distance accuracy estimations in an experiment with 18 participants was performed using the same protocols used in the first experiment. We compared this approach with the improved field of view with the previous three models we suggested in our first contribution. The results have demonstrated that the newly developed approach increased the previous results estimations by 11%. The estimation accuracy was improved from 80% to 91% based on mean absolute error calculations and the estimation error was reduced from 1.29% to 0.56%. These results showed that the real VR content system developed provides a strong starting point for the development of even more efficient methods and system requirements to improve distance accuracy for real VR content systems.

The new developed approach (Real + HMD + FOV) performed better than the previous two models developed in the first contribution (real + HMD and photo + HMD models). These results proved that the mismatch between the FOV of the VR displays and the cameras systems and the restricted FOV of the VR displays has a great impact on distance estimations of real VR content. Thus, improving the FOV improved dramatically distance estimations in the real VR content. This thesis results presents strong evidence of the need for novel distance estimation improvements methods for real world VR content systems and provided effective initial work towards this goal.

Future work

VR has more potentials and challenges to tackle before one can use it for tasks and activities applicable to the real world. With this thesis findings, we hope that this work encourages the use and development of real VR content, especially, that this is such a thrilling and

compelling research area in both academia and industry. Possible future research would be to study and improve the different depth cues to enhance distance estimation in VR when using video. This thesis proved that FOV is an important factor in improving distance estimations. Other features and depth cues could also be factors impacting distance compression and should be studied and understood to improve distance estimation in real environment rendering for VR. Another possible avenue will be to extend the camera setup to use 3 or more cameras, to validate more the results of the distance estimation performance with the two-camera set up.

From the results of this work, in all environments with blind walking the level of underestimation increased with increasing distances. However, for verbal reporting, the level of underestimations was variable among the different environments. Verbal reporting results were more variable than blind walking results. We also noticed how the estimation is highly variable among participants using verbal report method. Therefore, verbal reporting does not seem very reliable as a protocol for judging distances. It would be interesting to try and test other distance judgment methods and compare their performance with blind walking and verbal report methods, such as perceptual matching method and open-loop action-based tasks. This will allow to prove and choose which distance judgment method is more adequate for real VR content.

Additionally, it may be possible to further improve this work by exploring the effects of long-term viewing of the video and check how far it could induce fatigue.

REFERENCES

[1] Mitchell, Jeffrey T. Living dangerously : Why some firefighters take risk on the job. 2018.

[2] J. M. Knapp and J. M. Loomis. Limited field of view of head mounted displays is not the cause of distance underestimation in virtual environments. Presence: Teleoperators & Virtual Environments, vol. 13, no. 5, pp. 572–577, 2004.

[3] P. Willemsen, A. A. Gooch, W. B. Thompson and S. H. Creem-Regehr. Effects of stereo viewing conditions on distance perception in virtual environments. Presence: Teleoper. Virtual Environ., vol. 17, pp. 91–101, Feb 2008.

[4] W. Thompson, P. Willemsen, A. Gooch, S. Creem-Regehr, J. Loomis, and A. Beall. Does the quality of the computer graphics matter when judging distances in visually immersive environments?. Presence: Teleoperators and Virtual Environments, vol. 13, pp. 560–571, October 2004.

[5] V. Interrante, B. Ries, and L. Anderson. Distance perception in immersive virtual environments, revisited. Proceedings of the IEEE Conference on Virtual Reality, p. 3–10, IEEE Computer Society, 2006.

[6] M. Mon-Williams and J. Tresilian. Ordinal depth information from accommodation. Ergonomics, vol. 43, pp. 391–404, April 2000.

[7] W. Thompson, R. Fleming, S. Creem-Regehr, and J. K. Stefanucci. Visual perception from a computer graphics perspective. CRC press, 2011.

[8] Chen, Z., Aksit, D.C., Huang, J., Jin, H. Six-Degree of Freedom Video Playback of a Single Monoscopic 360-Degree Video. U.S. Patents 10368047B2, 30 July 2019.

[9] Gerval J.P., Popovici M., Ramdani M., El Kalai O., Boskoff V. and Tisseau J. Virtual Environments for Children. Proceedings International Conference on Computers and Advanced Technology Education (CATE), Cancun, Mexico, 416-420, 2000.

[10] Fatima El Jamiy and Ronald Marsh. A Survey on Depth Perception in Head Mounted Displays: Distance Estimation in Virtual Reality, Augmented Reality and Mixed Reality. IET Image Processing, 8pp, 2019.

[11] M. Auvray and P. Fuchs. Perception, immersion et interaction sensorimotrices en environnement virtuel. Realite virtuel Cognition, vol. 45, no. 1, pp. 23–35, 2007.

[12] Milgram, P., and Kishino, F. A taxonomy of mixed reality visual displays. IEICE TRANSACTIONS on Information and Systems, 77(12), 1321–1329, 1994.

[13] J.M. Loomis and J.M. Knapp. Virtual and Adaptive Environments : Applications, Implications, and Human Performance Issues, chapter Visual Perception of Egocentric Distance in Real and Virtual Environments, Laurence Erlbaum Associates, NJ, USA, pages 21–46, 2003.

[14] A. Murgia and P.M. Sharkey. Estimation of Distances in Virtual Environments Using Size Constancy. The International Journal of Virtual Reality, 1(8) :67–74, 2009.

[15] P. Fuchs. Interfaces Visuelles. Techniques de l'Ingénieur, (TE5906). ISSN 1632-3823, 2003.

[16]   S.H. Creem-Regehr, P. Willemsen, A.A. Gooch, and W.B. Thompson. The Influence of Restricted Viewing Conditions on Egocentric Distance Perception : Implications for Real and Virtual Environments. Perception, 34(2) :191–204, 2005.

[17]   E. Klein, J.E. Swan, G.S. Schmidt, M.A. Livingston, and O.G. Staadt. Measurement Protocols for Medium-Field Distance Perception in Large-Screen Immersive Displays. In IEEE Virtual Reality Conference, VR'2009, pages 107–113, Lousiana, USA, March 14– 18 2009.

[18]   B. Wu, T.L. Ooi, and Z.J. He. Perceiving Distance Accurately by a Directional Process of Integrating Ground Information. Nature, 428 :73–77, 2004.

[19]   J.M. Plumert, J.K. Kearney, J.F. Cremer, and K. Recker. Distance Perception in Real and Virtual Environments. ACM Transactions on Applied Perception (TAP), 2(3) :216–233, 2005.

[20]   P. Willemsen and A.A. Gooch. Perceived Egocentric Distances in Real, Image-Based, and Traditional Virtual Environments. In Proc of the IEEE Virtual Reality Conf., pages 275–276, 2002.

[21]   J M Loomis, R L Klatzky, J W Philbeck, and R Gvariabil Golledge. Assessing Auditory Distance Perception Using Perceptually Directed Action. Perception & Psychophysics, 60(6) :966–980, 1998.

[22]   P. Zahorik. Estimating Sound Source Distance With and Without Vision. Optometry & Vision Science, 78(5) :270–275, 2001.

[23]   J.A. Da Silva. Scales for Perceived Egocentric Distance in a Large Open Field : Comparison of Three Psychophysical Methods. The American Journal of Psychology, 98(1) :119–144,1985.

[24]   G. Békésy and E.G. Wever. Experiments in Hearing. McGraw-Hill, Oxford, England, 1960.

[25]   J.E. Cutting and P.M. Vishton. Perception of Space and Motion, chapter Perceiving Layout and Knowing Distances : The Integration, Relative Potency, and Contextual Use of Different Information about Depth, pages 69–117. Academic Press, New-York, USA, 1995.

[26]   Nitish Padmanabana, Robert Konrada, Tal Stramera, Emily A. Cooperb, and Gordon Wetzsteina. Optimizing virtual reality for all users through gaze-contingent and adaptive focus displays. Edited by Wilson S. Geisler, The University of Texas at Austin, Austin, TX, January 6, 2017.

[27]   Robert Konrad, Terry Kong. Depth Cues in VR Head Mounted Displays with Focus Tunable Lenses. Stanford University, 2015.

[28]   A. Dünser, R. Grasset, and M. Billinghurst. A Survey of Evaluation Techniques used in Augmented Reality Studies. Human Interface Technology Laboratory New Zealand, 2008.

[29]   Morgan, M. W. Relationship between accommodation and convergence. Archives of Ophthalmology, 47(6), 745–759, 1952.

[30]   R. Patterson. Human Factors of 3-D Displays. The Journal of the Society for Information Display, 15(11) :861–871, 2007.

[31]   M.S. Landy, L.T. Maloney, E.B. Johnston, and M. Young. Measurement and Modeling of Depth Cue Combination : In Defense of Weak Fusion. Vision Research, 35(3) :389–412, 1995.

[32]   C. Spence. Audiovisual Multisensory Integration. Acoustical Science and Technology, 28 (2) :61–70, 2007.

[33]   J.W. Philbeck and J.M. Loomis. Comparison of Two Indicators of Perceived Egocentric Distance under Full-Cue and Reduced-Cue Conditions. Journal of Experimental Psychology : Human Perception and Performance, 23(1) :72–85, 1997.

[34]   J. Andre and S. Rogers. Using Verbal and Blind-Walking Distance Estimates to Investigate the Two Visual Systems Hypothesis. Attention, Perception, & Psychophysics, 68(3) : 353–361, 2006.

[35]   D. Waller, and A. R. Richardson. Correcting distance estimates by interacting with immersive virtual environments: Effects of task and available sensory information. Journal of Experimental Psychology. Applied, 14 (1), 61–72, 2008.

[36]   J. M. Loomis and J. W. Philbeck. Measuring spatial perception with spatial updating and action. In M. Behrmann, R. L. Klatzky, & B. Macwhinney (Eds.), Embodiment, ego-space, and action (pp. 1–43). New York, NY: Psychology Press., 2008.

[37]   A. S. Gilinsky. Perceived size and distance in visual space. Psychological Review, 58 (6), 460–482, 1951.

[38]   B. Bodenheimer, J. Meng, H. Wu, G. Narasimham, B. Rump, T. P. McNamara, T. H. Carr, and J.J. Rieser. Distance estimation in virtual and real environments using bisection. In R. Fleming & M. Langer (Eds.), Proceedings of the 4th Symposium on Applied Perception in Graphics and Visualization, pp. 35–40, ACM Press, 2007.

[39]   J. Purdy and E. J. Gibson. Distance judgment by the method of fractionation. Journal of Experimental Psychology, 50 (6), 374–380, 1955.

[40]   J. J. Rieser, D. H. Ashmead, C. R. Talor, and G. A. Youngquist. Visual perception
        and the guidance of locomotion without vision to previously seen targets. Perception,
        19 (5), 675–689, 1990.

[41]   J. S. Lappin, A. L. Shelton, and J. J. Rieser. Environmental context influences
        visually perceived distance. Perception & Psychophysics, 68 (4), 571–581, 2006.

[42]   M. Berning, D. Kleinert, T. Riedel, and M. Beigl. A study of depth perception in
        hand-held augmented reality using autostereoscopic displays. In Proceedings of the
        International Symposium on Mixed and Augmented Reality (ISMAR) 2014, pages 93–
        98. IEEE, 2014.

[43]   I. P. Howard and B. J. Rogers. Seeing in depth, volume 2: Depth perception.
        Ontario, Canada: I. Porteous, 2002.

[44]   B. G. Witmer and W. J. Sadowski. Nonvisually Guided Locomotion to a Previously
        Viewed Target in Real and Virtual Environments. Human Factors: The Journal of the
        Human Factors and Ergonomics Society, 40(3):478–488, 1998.

[45]   P. Willemsen, M. B. Colton, S. H. Creem-Regehr, and W. B. Thompson. The
        Effects of Head-mounted Display Mechanics on Distance Judgments in Virtual
        Environments. In Proceedings of the Symposium for Applied Perception in Graphics
        and Visualization ACM, pages 35–38, New York, NY, USA, 2004.

[46]   J. M. Foley, N. P. Ribeiro-Filho, and J. A. D. Silva. Visual perception of extent and
        the geometry of visual space. Vision Res, vol. 44, no. 2, pp. 147–156, Jan 2004.

[47]   Azuma, R. A survey of augmented reality. In Presence: Teleoperators and Virtual
        Environments, 6(4):355–385, 1997.

[48]   J. E. Swan, A. Jones, E. Kolstad, M. A. Livingston, and H. S. Smallman. Egocentric Depth Judgments in Optical, See-through Augmented Reality. IEEE Transactions on Visualization and Computer Graphics, 13(3):429–442, 2007.

[49]   M. A. Livingston, A. Dey, C. Sandor, and B. H. Thomas. Pursuit of "X-ray vision" for Augmented Reality. In Human Factors in Augmented Reality Environments, pages 67–107, 2013.

[50]   J. E. Swan II, L. Kuparinen, S. Rapson, and C. Sandor. Visually Perceived Distance Judgments: Tablet-Based Augmented Reality Versus the Real World. International Journal of Human–Computer Interaction, pages 1–16, 2017.

[51]   J. W. McCandless, S. R. Ellis, and B. D. Adelstein. Localization of a Time-delayed, Monocular Virtual Object Superimposed on a Real Environment. Presence, 9(1):15–24, 2000.

[52]   J. P. Rolland, C. Meyer, K. Arthur, and E. Rinalducci. Method of Adjustments versus Method of Constant Stimuli in the Quantification of Accuracy and Precision of Rendered Depth in Head-Mounted Displays. Presence: Teleoperators and Virtual Environments, 11(6):610–625, 2002.

[53]   M. E. C. Santos, I. de Souza Almeida, G. Yamamoto, T. Taketomi, C. Sandor, and H. Kato. Exploring Legibility of Augmented Reality X-ray. Multimedia Tools and Applications, 75(16):9563–9585, 2016.

[54]   S. R. Ellis and B. M. Menges. Localization of Virtual Objects in the Near Visual Field. Human Factors: The Journal of the Human Factors and Ergonomics Society, 40(3):415–431, 1998.

[55]   Huang, J.M., Ong, S.K., Nee, A.Y.C. Real-time finite element structural analysis in augmented reality. Adv. Eng. Softw, 87, 43–56, 2015.

[56]   Huang, J.M., Ong, S.K., Nee, A.Y.C. Visualization and interaction of finite element analysis in augmented reality. Comput. Aided Des., 84, 1–14, 2017.

[57]   Weidlich, D., Scherer, S.,Wabner, M. Analyses using VR/AR visualization. IEEE Comput. Graph. Appl, 28, 84–86, 2008.

[58]   M. A. Cidota, R. M. Cli_ord, S. G. Lukosch, and M. Billinghurst. Using Visual Effects to Facilitate Depth Perception for Spatial Tasks in Virtual and Augmented Reality. In Proceedings of the International Symposium on Mixed and Augmented Reality (ISMAR) 2016, pages 172–177, 2016.

[59]   Vincent Couture, Michael S. Langer, and Sebastien Roy. 2011. Panoramic stereo video textures. In ICCV. 1251–1258, 2011.

[60]   Fan Zhang and Feng Liu. Casual stereoscopic panorama stitching. In CVPR. 2002–2010.

[61]   Peter Hedman, Suhib Alsisan, Richard Szeliski, and Johannes Kopf. Casual 3D photography. TOG (SIGGRAPH Asia) 36, 6 (2017), 234:1–234, 2017.

[62]   Rajiv Gupta and Richard I. Hartley. Linear pushbroom cameras. TPAMI 19, 963–975, 1997.

[63]   Christian Richardt, Yael Pritch, Henning Zimmer, and Alexander Sorkine-Hornung. 2013. Megastereo: Constructing high-resolution stereo panoramas. In CVPR. 1256–1263, 2013.

[64]   Shmuel Peleg, Moshe Ben-Ezra, and Yael Pritch. Omnistereo: Panoramic stereo imaging. TPAMI 23, 3 (2001), 279–290, 2001.

[65]   Shmuel Peleg and Moshe Ben-Ezra. Stereo panorama with a single camera. In CVPR. 1395–1401, 1999.

[66]   Steven M. Seitz and Jiwon Kim. The space of all stereo images. IJCV 48, 1 (2002), 21–38, 2002.

[67]   Heung-Yeung Shum, King To Ng, and Shing-Chow Chan. A virtual reality system using the concentric mosaic: Construction, rendering, and data compression. IEEE Transactions on Multimedia 7, 1 (2005), 85–95, 2005.

[68]   Vincent Chapdelaine-Couture and Sebastien Roy. The omnipolar camera: A new approach to stereo immersive capture. In ICCP. 1–9, 2013.

[69]   L. Arora and A. Joglekar. Cell phone controlled robot with fire detection sensors. (IJCSIT) International Journal of Computer Science and Information Technologies, vol. 6, no. 3, pp. 2954–2958, 2015.

[70]   El Jamiy, Fatima, Ananth N. Ramaseri Chandra, and Ronald Marsh. Distance accuracy of real environments in virtual reality head-mounted displays. IEEE International Conference on Electro Information Technology (EIT). IEEE, 2020.

[71]   F. El Jamiy and R. Marsh. Distance Estimation In Virtual Reality And Augmented Reality: A Survey. In 2019 IEEE International Conference on Electro Information Technology (EIT), pp. 063–068, IEEE, 2019.

[72]   Tan, L., Wang, Y., Yu, H., Zhu, J. Automatic camera calibration using active displays of a virtual pattern. Sensors 2017, 17, 685, 2017.

[73]   Qu, Z., Lin, S.-P., Ju, F.-R., Liu, L. The improved algorithm of fast panorama stitching for image sequence and reducing the distortion errors. Math. Probl. Eng. 2015.

[74] Rublee, E., Rabaud, V., Konolige, K., Bradski, G. ORB: An efficient alternative to SIFT or SURF. In Proceedings of the 2011 International conference on computer vision, Barcelona, Spain, pp. 2564–2571, November 2011.

[75] Jeon, H.-k., Jeong, J.-m., Lee, K.-y. An implementation of the real-time panoramic image stitching using ORB and PROSAC. In Proceedings of the 2015 International SoC Design Conference (ISOCC), Gyungju, South Korea, 2–5, pp. 91–92, november 2015.

[76] Wang, M., Niu, S., Yang, X. A novel panoramic image stitching algorithm based on ORB. In Proceedings of the 2017 International Conference on Applied System Innovation (ICASI), Sapporo, Japan, pp. 818–821, May 2017.

[77] Brown, M., Lowe, D.G. Automatic panoramic image stitching using invariant features. Int. J. Comput. Vis., 59–73, 2017.

[78] Din, I., Anwar, H., Syed, I., Zafar, H., Hasan, L. Projector calibration for pattern projection systems. J. Appl. Res. Technol., 2014.

[79] Pandey, A., Pati, U.C. A novel technique for non-overlapping image mosaicing based on pyramid method. In Proceedings of the 2013 Annual IEEE India Conference (INDICON), Mumbai, India, pp. 1–6, December 2013.

[80] Chaudhari, K., Garg, D., Kotecha, K. An enhanced approach in Image Mosaicing using ORB Method with Alpha blending technique. Int. J. Adv. Res. Comput. Sci., 8, 917–921, 2017.

[81] Dessein, A., Smith,W.A., Wilson, R.C., Hancock, E.R. Seamless texture stitching on a 3D mesh by Poisson blending in patches. In Proceedings of the 2014 IEEE

International Conference on Image Processing (ICIP), Paris, France, pp. 2031–2035, 27–30 October 2014.

[82] Allène, C., Pons, J.-P., Keriven, R. Seamless image-based texture atlases using multi-band blending. In Proceedings of the 2008 19th International Conference on Pattern Recognition, Tampa, FL, USA, pp. 1–4, December 2008.

[83] Burt, P.J., Adelson, E.H. A multiresolution spline with application to image mosaics. Acm Trans. Graph. (TOG), 217–236, 1983.

[84] Matt Yu, Haricharan Lakshman, Bernd Girod. Content Adaptive Representations of Omnidirectional Videos for Cinematic Virtual Reality. ImmersiveME '15: Proceedings of the 3rd International Workshop on Immersive Media Experiences, Pages 1–6, October 2015.

[85] KK Gillingham. A primer of vestibular function, spatial disorientation, and motion sickness. Aeromedical Reviews, 1966

[86] Stephan Reichelt, Ralf Häussler, Gerald Fütterer, and Norbert Leister. Depth cues in human visual perception and their realization in 3D displays. Proc. SPIE 7690, Three-Dimensional Imaging, Visualization, and Display 2010 and Display Technologies and Applications for Defense, Security, and Avionics IV, 76900B, 14 May 2010.

[87] Mi Posner, Gj Digirolamo. Cognitive neuroscience: Origins and promise - Psychological bulletin, 2000.

[88] Karrasch, Pierre, and Sebastian Hunger. Simulation of vegetation and relief induced shadows on rivers with remote sensing data. Earth Resources and

Environmental Remote Sensing/GIS Applications VIII. Vol. 10428. International Society for Optics and Photonics, 2017.

[89]   Stenglin, Maree Kristen. Space odyssey: Towards a social semiotic model of three-dimensional space. Visual Communication 8.1: 35-64, 2009.

[90]   Crary, Jonathan. Techniques of the Observer. Cambridge, MA: MIT press, 1990.

[91]   Gogel, Walter C. Size, distance, and depth perception. Perceptual Processing. Academic Press, 299-333, 1978.

[92]   Hammad, Sherief. Components of optical information for depth induce a picture-surface angle illusion. University of Toronto (Canada), 2015

[93]   Hashimoto, Naoki, and Masayuki Nakajima. View-dependent focal blur in immersive virtual environments. Proc. the 10th International Conference on Artificial Reality and Telexistence, 2000.

[94]   Proffitt, Dennis R., and Corrado Caudek. Depth perception and the perception of events. 2003.

[95]   Tuan, Yi-Fu. Topophilia: A study of environmental perception, attitudes, and values. Columbia University Press, 1990.

[96]   Zia, O., Kim, J.H., Han, K., Lee, J.W. 360° Panorama Generation using Drone Mounted Fisheye Cameras. In Proceedings of the 2019 IEEE International Conference on Consumer Electronics (ICCE), Las Vegas, NV, USA, pp. 1–3, January 2019.

[97]   Gledhill D., Tian G. Y., Taylor D., Clarke D., Panoramic imaging - a review. Computers and Graphics, 27 (3). pp. 435-445, 2003

[98]   Xiong, Yalin, and Kenneth Turkowski. Creating image-based VR using a self-calibrating fisheye lens. Proceedings of IEEE computer society conference on computer vision and pattern recognition. IEEE, 1997.

[99]   Scaramuzza, Davide, and Katsushi Ikeuchi. Omnidirectional camera. (2014): 552-560, 2014.

[100]   Wang, Ke, et al. Dioptric Fisheye Panoramic Camera Calibration Based on Unifying Spherical Projection Model. Applied Mechanics and Materials. Vol. 268. Trans Tech Publications Ltd, 2013.

[101]   Nayar, Shree K. Catadioptric omnidirectional camera. Proceedings of IEEE computer society conference on computer vision and pattern recognition. IEEE, 1997.

[102]   Yong, H. Huang, J. Xiang,W., Hua, X., Zhang, L. Panoramic background image generation for PTZ cameras. IEEE Trans. Image Process., 28, 3162–3176, 2019.

[103]   Ivo Dinov. F-Distribution Tables - Statistics Online Computational Resource. http://www.socr.ucla.edu/Applets.dir/F_Table.html. Last accessed 3/16/2022.

APPENDICES

```
211
212     for_each_eye([&](ovrEyeType eye){
213         EyeArgs & eyeArgs = perEyeArgs[eye];
214         ovrTextureHeader & eyeTextureHeader = eyeArgs.textures.OGL.Header;
215         eyeFovPorts[eye] = hmdDesc.DefaultEyeFov[eye];
216         eyeTextureHeader.TextureSize = ovrHmd_GetFovTextureSize(hmd, eye, hmdDesc.DefaultEyeFov[eye], 1.0f);
217         eyeTextureHeader.RenderViewport.Size = eyeTextureHeader.TextureSize;
218         eyeTextureHeader.RenderViewport.Pos.x = 0;
219         eyeTextureHeader.RenderViewport.Pos.y = 0;
220         eyeTextureHeader.API = ovrRenderAPI_OpenGL;
221
222         imageTextures[eye] = TexturePtr(new Texture());
223         imageTextures[eye]->bind();
224         imageTextures[eye]->parameter(GL_TEXTURE_MAG_FILTER, GL_LINEAR);
225         imageTextures[eye]->parameter(GL_TEXTURE_MIN_FILTER, GL_LINEAR);
226         glTexImage2D(GL_TEXTURE_2D, 0, GL_RGB, RENDER_IMAGE_WIDTH, RENDER_IMAGE_HEIGHT, 0, GL_BGR, GL_UNSIGNED_BYTE, 0x0000);
227
228         perEyeReadImage[eye] = cvCreateImage(cvSize(CAM_IMAGE_WIDTH, CAM_IMAGE_HEIGHT), 8, 3);
229         perEyeWriteImage[eye] = cvCreateImage(cvSize(CAM_IMAGE_WIDTH, CAM_IMAGE_HEIGHT), 8, 3);
230
231         eyeArgs.framebuffer.init(Rift::fromOvr(eyeTextureHeader.TextureSize));
232         eyeArgs.textures.OGL.TexId = eyeArgs.framebuffer.color->texture;
233     });
234
235
236 .................
237
238
239
240     int distortionCaps = ovrDistortionCap_TimeWarp | ovrDistortionCap_Chromatic | ovrDistortionCap_Vignette | ovrDistortionCap_NoSwapBuffers;
241
242
243     ovrEyeRenderDesc eyeRenderDescs[2];
244     int configResult = ovrHmd_ConfigureRendering(hmd, &cfg.Config,
245                                                  distortionCaps, eyeFovPorts, eyeRenderDescs);
246
247     for_each_eye([&](ovrEyeType eye){
248         EyeArgs & eyeArgs = perEyeArgs[eye];
249         eyeArgs.projection = Rift::fromOvr(
250         ovrMatrix4f_Projection(eyeFovPorts[eye], 0.01, 100, true));
251 });
252
```

```cpp
30
31  static bool CamCalibration(Size& imgSize, Mat& camMatrix, Mat& distanceCoefs,
32    vector<vector<Point2f> > imgPoints, vector<Mat>& rvs, vector<Mat>& tvs,
33    vector<float>& reprojectionErrs, double& sumAvgErr)
34  {
35
36    camMatrix = Mat::eye(3, 3, CV_64F);
37    if (flagParam & CV_CALIB_FIX_ASPECT_RATIO)
38      camMatrix.at<double>(0, 0) = 1.0;
39
40    distanceCoefs = Mat::zeros(8, 1, CV_64F);
41
42    vector<vector<Point3f> > objPoints(1);
43    computeBoardCornerPositions(boardSizeParam, squareSizeParam, objPoints[0], calibrationPatternParam);
44
45    objPoints.resize(imgPoints.size(), objPoints[0]);
46
47    // intrinsic and extrinsic camera parameters
48    double re = calibrateCamera(objPoints, imgPoints, imgSize, camMatrix,
49      distanceCoefs, rvs, tvs, flagParam | CV_CALIB_FIX_K4 | CV_CALIB_FIX_K5);
50
51
52    bool chRange = checkRange(camMatrix) && checkRange(distanceCoefs);
53
54    sumAvgErr = calcReprojectionErrors(objPoints, imgPoints,
55      rvs, tvs, camMatrix, distanceCoefs, reprojectionErrs);
56
57    return chRange;
58  }
59
```

```
142
143  void homographyWarping(map<vector<float>, VlSiftKeypoint> &features,
144      Homography Homogr, float x, float y) {
145      map<vector<float>, VlSiftKeypoint>::iterator it = features.begin();
146      for (it; it != features.end(); ++it) {
147          float xPoint = it->second.x;
148          float yPoint = it->second.y;
149          it->second.x = get_warped_x(xPoint, yPoint, Homogr) - x;
150          it->second.y = get_warped_y(xPoint, yPoint, Homogr) - y;
151          it->second.i_x = int(it->second.x);
152          it->second.i_y = int(it->second.y);
153      }
154  }
155
```

Appendix D
ANOVA Analysis - blind walking - distance 7m

	G1	x-mean	(x-mean)2	G2	x-mean	(x-mean)2	G3	x-mean	(x-mean)2	G4	x-mean	(x-mean)2
	5.25	-0.815	0.664	2.5	-2.372	5.625	3.86	-3.256	10.602	3	-2.842	8.075
	5.4	-0.665	0.442	4.2	-0.672	0.451	4.9	-2.216	4.911	5.5	-0.342	0.117
	5.82	-0.245	0.060	2.75	-2.122	4.501	4.9	-2.216	4.911	4.5	-1.342	1.800
	5.17	-0.895	0.801	3.3	-1.572	2.470	7.1	-0.016	0.000	5.5	-0.342	0.117
	7	0.935	0.874	6.4	1.528	2.336	8.9	1.784	3.182	5.15	-0.692	0.478
	6.15	0.085	0.007	4.55	-0.322	0.103	8.6	1.484	2.202	8.5	2.658	7.067
	5.8	-0.265	0.070	6.71	1.838	3.379	6.5	-0.616	0.380	4	-1.842	3.392
	5.61	-0.455	0.207	4.55	-0.322	0.103	5	-2.116	4.478	6.8	0.958	0.918
	5.85	-0.215	0.046	6	1.128	1.273	9	1.884	3.549	5.5	-0.342	0.117
	6	-0.065	0.004	5.4	0.528	0.279	5.55	-1.566	2.453	6	0.158	0.025
	7.72	1.655	2.739	6.6	1.728	2.987	8.15	1.034	1.069	6.2	0.358	0.128
	6.4	0.335	0.112	7.1	2.228	4.965	6.7	-0.416	0.173	5.5	-0.342	0.117
	5.2	-0.865	0.748	2.6	-2.272	5.160	6.45	-0.666	0.444	6.7	0.858	0.737
	5.73	-0.335	0.112	2.83	-2.042	4.168	10.46	3.344	11.182	7.5	1.658	2.750
	6.1	0.035	0.001	3.85	-1.022	1.044	6.75	-0.366	0.134	6.7	0.858	0.737
	5.94	-0.125	0.016	6.7	1.828	3.343	9.47	2.354	5.541	5.8	-0.042	0.002
	6.35	0.285	0.081	5.85	0.978	0.957	9.35	2.234	4.990	5.8	-0.042	0.002
	7.68	1.615	2.608	5.8	0.928	0.862	6.45	-0.666	0.444	6.5	0.658	0.433
sum	109.17	9.8E-15	9.595	87.69	9E-15	44.009	128.1	-5E-15	60.644	105.2	-2E-15	27.0113
mean	6.065			4.872			7.116			5.842		

Appendix E
ANOVA Analysis - F-Test - blind walking - distance 7m

SSW	141.259						
	Observations	x-mean	(x-mean)²				
	5.25	-0.724	0.524		Total sum of squares	187.076	
	5.4	-0.574	0.329		Sum of squares within	141.259	
	5.82	-0.154	0.024		Sum of squares between	45.816	
	5.17	-0.804	0.646				
	7	1.026	1.053		Degrees of freedom		
	6.15	0.176	0.031		Numerator	3	
	5.8	-0.174	0.030		Denominator	68	
	5.61	-0.364	0.132				
	5.85	-0.124	0.015				15.272
	6	0.026	0.001				2.077
	7.72	1.746	3.050				
	6.4	0.426	0.182		F		7.352
	5.2	-0.774	0.598		p-value		0.00024
	5.73	-0.244	0.059				
	6.1	0.126	0.016				
	5.94	-0.034	0.001		F(3,68) = 2.74		
	6.35	0.376	0.142				
	7.68	1.706	2.912				F Cal > F table ==> REJECT
	2.5	-3.474	12.066				
	4.2	-1.774	3.146				
	2.75	-3.224	10.392				
	3.3	-2.674	7.148				
	6.4	0.426	0.182				
	4.55	-1.424	2.027				
	6.71	0.736	0.542				
	4.55	-1.424	2.027				
	6	0.026	0.001				
	5.4	-0.574	0.329				
	6.6	0.626	0.392				
	7.1	1.126	1.269				
	2.6	-3.374	11.381				
	2.83	-3.144	9.882				
	3.85	-2.124	4.510				
	6.7	0.726	0.528				
	5.85	-0.124	0.015				
	5.8	-0.174	0.030				
	3.86	-2.114	4.467				
	4.9	-1.074	1.153				
	4.9	-1.074	1.153				
	7.1	1.126	1.269				
	8.9	2.926	8.564				
	8.6	2.626	6.898				
	6.5	0.526	0.277				
	5	-0.974	0.948				
	9	3.026	9.159				
	5.55	-0.424	0.179				
	8.15	2.176	4.737				
	6.7	0.726	0.528				
	6.45	0.476	0.227				
	10.46	4.486	20.128				
	6.75	0.776	0.603				
	9.47	3.496	12.225				
	9.35	3.376	11.400				
	6.45	0.476	0.227				
	3	-2.974	8.842				
	5.5	-0.474	0.224				
	4.5	-1.474	2.172				
	5.5	-0.474	0.224				
	5.15	-0.824	0.678				
	8.5	2.526	6.383				
	4	-1.974	3.895				
	6.8	0.826	0.683				
	5.5	-0.474	0.224				
	6	0.026	0.001				
	6.2	0.226	0.051				
	5.5	-0.474	0.224				
	6.7	0.726	0.528				
	7.5	1.526	2.330				
	6.7	0.726	0.528				
	5.8	-0.174	0.030				
	5.8	-0.174	0.030				
	6.5	0.526	0.277				
MEAN	5.974						
		SUM	187.076				

Appendix F
ANOVA Analysis - blind walking - distance 9m

	G1	x-mean	(x-mean)2	G2	x-mean	(x-mean)2	G3	x-mean	(x-mean)2	G4	x-mean	(x-mean)2
	6.2	-1.532	2.346	2.75	-3.441	11.841	4.35	-2.654	7.043	7	-0.474	0.225
	7.6	-0.132	0.017	6	-0.191	0.037	5.55	-1.454	2.114	7	-0.474	0.225
	7.5	-0.232	0.054	4.7	-1.491	2.223	4.98	-2.024	4.096	6.5	-0.974	0.950
	7.01	-0.722	0.521	5.17	-1.021	1.043	6.55	-0.454	0.206	7.1	-0.374	0.140
	9.25	1.518	2.305	2.65	-3.541	12.539	10.85	3.846	14.793	7.02	-0.454	0.207
	7.9	0.168	0.028	5.51	-0.681	0.464	8.4	1.396	1.949	9	1.526	2.327
	8.15	0.418	0.175	7.93	1.739	3.024	5.87	-1.134	1.286	5.5	-1.974	3.898
	7.71	-0.022	0.000	6.45	0.259	0.067	8	0.996	0.992	5	-2.474	6.123
	6.9	-0.832	0.692	7.27	1.079	1.164	9.5	2.496	6.231	7.4	-0.074	0.006
	8	0.268	0.072	4.85	-1.341	1.799	7.7	0.696	0.485	8.1	0.626	0.391
	8.95	1.218	1.484	7.65	1.459	2.128	9.45	2.446	5.983	8.1	0.626	0.391
	8.2	0.468	0.219	8.53	2.339	5.470	8.78	1.776	3.155	7.5	0.026	0.001
	6.4	-1.332	1.773	3.45	-2.741	7.514	6.55	-0.454	0.206	10.2	2.726	7.429
	7.93	0.198	0.039	5.88	-0.311	0.097	6.84	-0.164	0.027	7.7	0.226	0.051
	8	0.268	0.072	8.12	1.929	3.721	8.65	1.646	2.710	8.3	0.826	0.682
	7.27	-0.462	0.213	7.78	1.589	2.525	5.2	-1.804	3.254	6.5	-0.974	0.950
	7.85	0.118	0.014	7.25	1.059	1.121	4.85	-2.154	4.639	8.12	0.646	0.417
	8.35	0.618	0.382	9.5	3.309	10.949	4	-3.004	9.023	8.5	1.026	1.052
SUM	139.2	-1.42109E	10.408	111.44	4.44089E	67.725	126.07	-1.243E	68.191	134.54	-2.5757E-14	25.463
MEAN	7.732			6.191			7.004			7.474		

ANOVA Analysis - F-Test - blind walking - distance 9m

SSW	171.7875					
	Observations	x-mean	(x-mean)²			
	6.2	-0.900	0.811	Total sum of squares	196.529	
	7.6	0.500	0.250	Sum of squares within	171.788	
	7.5	0.400	0.160	Sum of squares between	24.741	
	7.01	-0.090	0.008			
	9.25	2.150	4.621	Degrees of freedom		
	7.9	0.800	0.640	Numerator		3
	8.15	1.050	1.102	Denominator		68
	7.71	0.610	0.372			
	6.9	-0.200	0.040			8.247
	8	0.900	0.810			2.526
	8.95	1.850	3.421			
	8.2	1.100	1.209	F		3.265
	6.4	-0.700	0.490	p-value		0.0266
	7.93	0.830	0.688			
	8	0.900	0.810			
	7.27	0.170	0.029	F(3,68) = 2.74		
	7.85	0.750	0.562			
	8.35	1.250	1.562			F Cal > F table ==> REJECT
	2.75	-4.350	18.925			
	6	-1.100	1.211			
	4.7	-2.400	5.761			
	5.17	-1.930	3.726			
	2.65	-4.450	19.805			
	5.51	-1.590	2.529			
	7.93	0.830	0.688			
	6.45	-0.650	0.423			
	7.27	0.170	0.029			
	4.85	-2.250	5.064			
	7.65	0.550	0.302			
	8.53	1.430	2.044			
	3.45	-3.650	13.325			
	5.88	-1.220	1.489			
	8.12	1.020	1.040			
	7.78	0.680	0.462			
	7.25	0.150	0.022			
	9.5	2.400	5.759			
	4.35	-2.750	7.564			
	5.55	-1.550	2.403			
	4.98	-2.120	4.496			
	6.55	-0.550	0.303			
	10.85	3.750	14.060			
	8.4	1.300	1.689			
	5.87	-1.230	1.514			
	8	0.900	0.810			
	9.5	2.400	5.759			
	7.7	0.600	0.360			
	9.45	2.350	5.521			
	8.78	1.680	2.821			
	6.55	-0.550	0.303			
	6.84	-0.260	0.068			
	8.65	1.550	2.402			
	5.2	-1.900	3.611			
	4.85	-2.250	5.064			
	4	-3.100	9.612			
	7	-0.100	0.010			
	7	-0.100	0.010			
	6.5	-0.600	0.360			
	7.1	0.000	0.000			
	7.02	-0.080	0.006			

	9	1.900	3.609		
	5.5	-1.600	2.561		
	5	-2.100	4.411		
	7.4	0.300	0.090		
	8.1	1.000	0.999		
	8.1	1.000	0.999		
	7.5	0.400	0.160		
	10.2	3.100	9.608		
	7.7	0.600	0.360		
	8.3	1.200	1.439		
	6.5	-0.600	0.360		
	8.12	1.020	1.040		
	8.5	1.400	1.959		
MEAN	7.100				
		SUM	196.529		